idocument title/ titre du document

Envisat Cyclic Altimetric Report

CYCLE 42 from 24-10-2005 to 28-11-2005

Quality Assessment Report

prepared by	Carolina Nogueira Loddo - SERCO
checked by	Gareth Davies - VEGA
approved by	Yannice Faugere - CLS
reference	ENVI-GSOP-EOPG-03-0011
issue	1
date of issue	06 December 2005
status	Reviewed
Document type	Technical Note

European Space Agency
Agence spatiale européenne

TABLE OF CONTENTS

1 INTRODUCTION

This documents aims at reporting on the performance of the EnviSat Radar Altimeter, Microwave Radiometer and DORIS sensors, on the data quality of the corresponding Fast Delivery products as well as on the main events which occurred during cycle 42.

This report covers the period from the 24th of October 2005 to the 28th of November.

2 DISTRIBUTION LIST

This report is available in PDF format at the internet address
http://earth.esa.int/pcs/envisat/ra2/reports/pcs_cyclic/

3 ACRONYMS

AGC	Automatic Gain Control
DORIS	Doppler Orbitography and Radiopositioning Integrated by Satellite
DSR	Data Set Record
EPC	Electronic Power Converter
ERS	European Remote Sensing satellite
ESRIN	European Space Research Institute
ESOC	European Space Operations Centre
FD	Fast Delivery products
GS	Ground Segment
GTS	Globa l Telecommunication System
HTL	Height Tracking Loop
ICU	Instrument Control Unit
IECF	Instrument Engineering Calibration Facility
IF	Intermediate Frequency
IE	Individual Echoes
IPF	Instrument Processing Facility
LUT	Look Up Table
MCMD	MacroCommand
MPH	Main Product Header
MSS	Mean Sea Surface
MWR	MicroWave Radiometer
MPS	Mission Planning System
NRT	Near Real Time
OBT	On-Board Time
OCM	Orbit Control Mode/Manoeuvres
PCS	ERS Products Control Service
PCF	EnviSat Product Control Facility
PDHS-E	ESRIN Processing and Data Handling Station

PDHS-K	Kiruna Processing and Data Handling Station
PLSOL	Payload Switch-Off Line
PMC	Payload Main Computer
PSO	On-orbit Position
PTR	Point Target Response
RA-2	EnviSat Radar Altimeter bi-frequency
RSL	Resolution Selection Logic
SAD	Static Auxiliary Files
SBT	Satellite Binary Time
SEU	Single Event
SFCM	Stellar Fine Control Mode
SPH	Specific Product header
SPSA	Signal Processing Sub-Assembly
SYSM	Stellar Yaw Steering Mode
S/W	Software
TM	Telemetry
TRP	Transponder
TWT	Traveling Wave Tube
UTC	Coordinated Universal Time
YSM	Yaw Stellar Mode

4 REFERENCE DOCUMENTS

[R – 1a] F-PAC MONTHLY REPORT, SALP-RP-M-OP-15389-CN, July 2005
[R – 1b] F-PAC MONTHLY REPORT, SALP-RP-M-OP-15387-CN, August 2005
[R – 2] ENVISAT Microwave Radiometer Assessment Report Cycle 042, CLS.DOS/05.147, http://earth.esa.int/pcs/envisat/mwr/reports/
[R – 3] Envisat RA-2 IF Mask weird behavior: Investigation Report
[R – 4] Instrument Performance Evaluation and Analysis Summary, PO-TR-ALS-RA-0042
[R – 5] Instrument Corrections Applied on RA-2 Level 1b products, Paper presented at the ENVISAT Calibration Review in September 2002
[R – 6] ENVISAT Phase E Cal/Val Acquisition Plan, ENVI-SPPA-EOPG-TN-03-0008
[R – 7] RA-2 S-Band Anomaly Investigation, PO-TN-ESA-RA-1342, http://earth.esa.int/pcs/envisat/ra2/articles/
[R – 8] RA-2 Performance Results, Paper presented at the ENVISAT Calibration Review in September 2002
[R – 9a] ECMWF Report on ENVISAT RA- 2 for July 2005, Report on ENVISAT Radar Altimeter - 2 (RA- 2), Wind/ Wave Product with Height Information (RA2_ WWV_ 2P),
[R – 9b] ECMWF Report on ENVISAT RA- 2 for August 2005, Report on ENVISAT Radar Altimeter - 2 (RA- 2), Wind/ Wave Product with Height Information (RA2_ WWV_ 2P), http://earth.esa.int/pcs/envisat/ra2/reports/ecmwf/
[R – 10] Envisat GDR Quality Assessment Report, SALP-RP-P2-EX-21121-CLS015
[R – 11] Envisat RA-2 Range Instrumental correction: USO clock period variations and associated auxiliary file, ENVI-GSEG-EOPG-TN-03-0009

[R – 12] Defining a Rain flag for the Envisat altimeter, G. Quartly, study presented to the final CCVT plenary meeting, http://earth.esa.int/pcs/envisat/ra2/articles/
[R – 13] ENVISAT Weekly Mission Operations Reports # 176-180, ENVI-ESOC-OPS-RP-1011-TOS-OF
[R – 14] Envisat validation and cross calibration activities during the verification phase. Synthesis Report ESTEC contract No. 16243/02/NL/FF WP6, http://earth.esa.int/pcs/envisat/ra2/articles/
[R – 15] ENVISAT-1 Products Specifications - Vol. 14: RA-2 Products Specifications, PO-RS-MDA-GS-2009, Iss 3, Rev. K, 24/05/2004
[R – 16] Algorithm for Flag identification and waveforms reconstruction of RA-2 data affected by “S-Band anomaly”, ENVI-GSEG-TN-04-0004, Issue 1.4
[R-17] Envisat Cyclic Report Cycle 28, ENVI-GSOP-EOPG-03-0011

5 GENERAL QUALITY ASSESSMENT

5.1 Cycle Overview

- New version of IPF processing chain, V5.02 installed in both PDHS-E and PDHS-K on October the 24th 2005.
- During cycle 42 the Radar Altimeter 2 was unavailable once, for a total of 3 orbits.
- Data availability is around 97%.
- The total percentage of data affected by the so called “S-Band anomaly” corresponds to about 2.4% of the acquired data.
- The number of valid IF masks is 19, which represents about 29% of the planned IF masks.
- Tracking performances in the different resolutions are well in line with the output figures and objectives of the Commissioning Phase.
- The USO clock period trend retrieved for cycle 42 shows a drift=-1.9 mm/year and a bias=22 mm.
- The MWR and DORIS were never unavailable, with data availability of 98% for MWR and almost 98% for DORIS.

5.2 Payload status

5.2.1 ALTIMETER EVENTS

The Radar Altimeter 2, during cycle 42, was unavailable once in the following time frame:

Start: 28 Oct 2005 05:34:13, Orbit = 19140
Stop: 28 Oct 2005 10:39:00, Orbit = 19143

Cause: RA-2 switched to Suspend due to an ‘uncontrolled software action’. This is a repeat of an anomaly that has been observed a few times before, and is under investigation (ref: AR ENV-774)

5.2.1.1 RA-2 instrument planning

The RA-2 instrument planning was performed as follows:

- IF Calibration Mode according to the nominal operational acquisition scheme: 100 seconds of data twice per day over Himalayan region (ascending and descending passes).
- Preset Loop Output mode for GAVDOS Range transponders, located in Creta.
- Preset Loop Output mode over the ESA transponder located in Rome (permanent location); high chirp resolution.
- Preset Loop Output and Individual Echoes acquisitions over the CryoSat transponder located in Svalbard; low chirp resolution.
- Individual Echoes background planning: the buffering of 20 Data Blocks of Individual Echoes (1.114 sec.) transmitted every 160 Data Blocks starts after flying over the Himalayan region (both ascending and descending passes) and is operated for half a day.
- Individual Echoes acquisitions during PLO activity over ESA transponder located in Rome (1 second length acquisition, 1 repetition)

Hereafter the map is reported showing the acquisition sites for both the Range and Sigma_0 transponders.

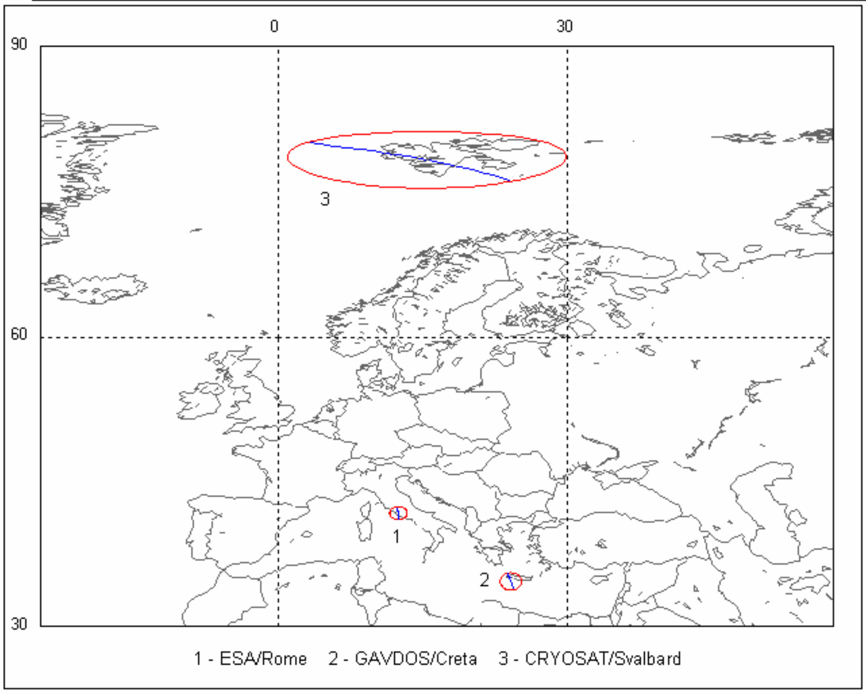

Figure 1: Transponder Acquisition sites for cycle 42

5.2.2 MWR EVENTS

The MWR, during cycle 42 was never unavailable [R-13].

5.2.3 DORIS EVENTS

The DORIS, during cycle 42 was never unavailable [R-13].

5.3 Availability

The summary of the RA-2 data products availability for this cycle is reported in Appendix 2.
Data availability was 97% for RA2 products, 98% for MWR and almost 98% for DORIS products.

5.4 Orbit quality

During cycle 42 no manoeuvre was executed. The orbit was maintained within the +/- 1km to the reference ground track during cycle 42.

5.5 Ground Segment Processing Chain Status

5.5.1 IPF PROCESSING CHAIN

5.5.1.1 Version

The current version of the IPF processing chain is V5.02, installed in both PDHS-E and PDHS-K on 24th October 2005. It contains the following algorithms and auxiliary data files upgrade:

1. USO instrumental correction within the RA-2 L1b processor.
2. New MWR Side Lobes correction algorithm within MWR L1b processor
3. Correction of the mispointing evaluation algorithm within the RA-2 L2 processor
4. Inclusion of the loading tide for the GOT2000.2 model.
5. Addition of the peakiness fields in Ku and S band to the RA-2 and MWR FD/I/MAR meteorological products
6. Inclusion of the square of the significant wave height in Ku and S band
7. Inclusion of an S-band anomaly flag, see [R – 16]
8. Upgrade of the Level 1B and Level 2 processing for DORIS NRT orbital information computation
9. New ADF for Digital Elevation Model (DEM): AUX_DEM_AX
10. Adjustment of the S Band computation for the rain flag
11. New ADF for wind table: RA2_SOI_AX

A new version of the IPF should be released at the beginning of next year in order to fix some discrepancies related to points 5 and 7. Given some planning problems encountered during cycle

42, point 8 could only be covered at the last part of the cycle, i.e. since the 21st of November products have been processed using DORIS NRT orbital information computation.

The previous IPF version V4.58 was operational at the Envisat PDHS-K and PDHS-E since 16th July 2004. A complete table of IPF Level1b and Level2 upgrades is reported in Appendix 1.

5.5.1.2 Auxiliary Data File

The Auxiliary files actually used by the IPF ground processing are reported in Appendix 3.
The RA2_USO_AX, RA2_POL_AX, the RA2_SOL_AX and the RA2_PLA_AX have been regularly updated every week without problems. The RA2_IFF_AX has been updated once.

The RA-2 Auxiliary Data Files (ADF) are accessible from the Envisat Web pages under http://www.envisat.esa.int/services/auxiliary_data/ra2mwr/ .

5.5.2 F-PAC PROCESSING CHAIN

The current version of CMA is V7.1 operational since 24th October 2005.
F-PAC CMA anomalies: anomalies are detailed in the F-PAC Monthly Report [R – 1a] and [R-1b].
The F-PAC CMA processing chain includes all the IPF evolutions plus some others like:
- Inclusion of GPS Ionospheric correction
- Inclusion of MOG2D Inverse Barometer Geophysical Correction in Level 2 products
- FES2004
- Addition of a field for Level 1B SW ID in Level 2 products
- Inclusion of nadir location not corrected for slope model

6 INSTRUMENT PERFORMANCE

6.1 RA-2 Performance

6.1.1 TRACKING CAPABILITY

The percentages of acquisition in the different resolutions subdivided by surface type are given in the Table bellow:

Surface type	320 MHz	Commissioning Phase objectives 320 MHz	80 MHz	20MHz
Open Ocean	99,99	>99%	0,01	0,00
Costal Water (ocean depth < 200 m)	98,36	No specific requirement	1,47	0,17
Sea Ice	99,26	>95%	0,67	0,08

Ice Sheet	96,41	>95%	2,89	0,70
Land	81,68	No specific requirement	13,39	4,93
All world	95,30		3,49	1,21

Table 1: RA-2 Tracking capability: Chirp ID percentages discriminated by surface type

The figures given for the RA-2 tracking performances during this cycle are very much in line with the ones recorded at the end of the Commissioning Phase reported in the last column and presented in [R – 8]. The slight differences are in part due to the different algorithms used to discriminate the surface types.
In Figure 2, Figure 3 and Figure 4 the cyclic tracking percentages for the three RA-2 bandwidths are reported.
The worsening in performance noticeable for cycle 20 was due to the up-load of wrong on-board software parameters which lasted for about three days.

In general, even if a tiny evolution can be observed, the tracking performances are well in line with the output figures and objectives of the Commissioning Phase as given in Table 1.

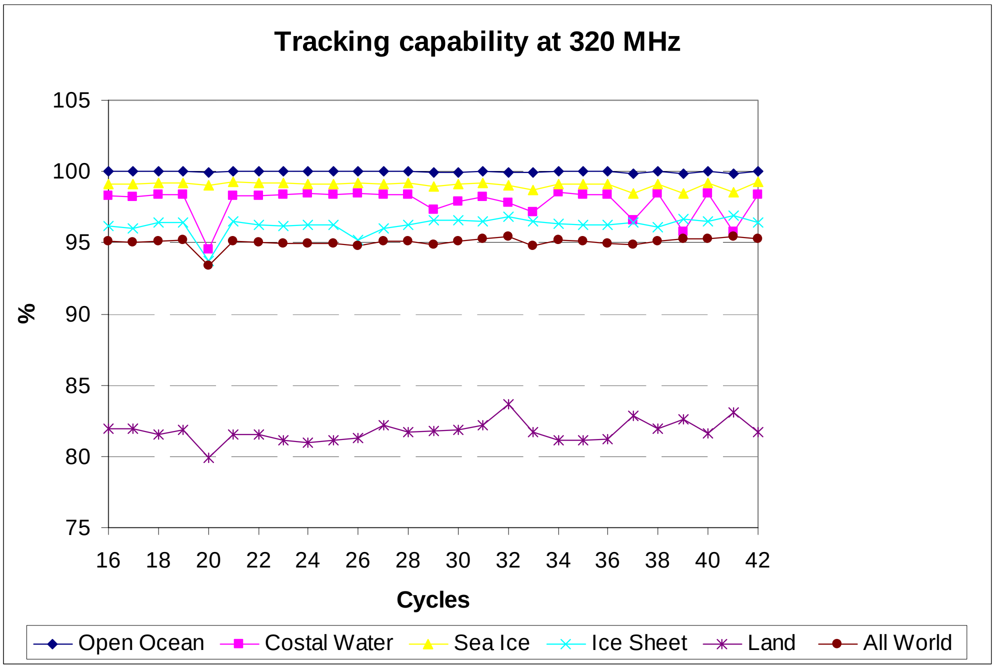

Figure 2: RA-2 Tracking percentage at 320MHz for different surfaces

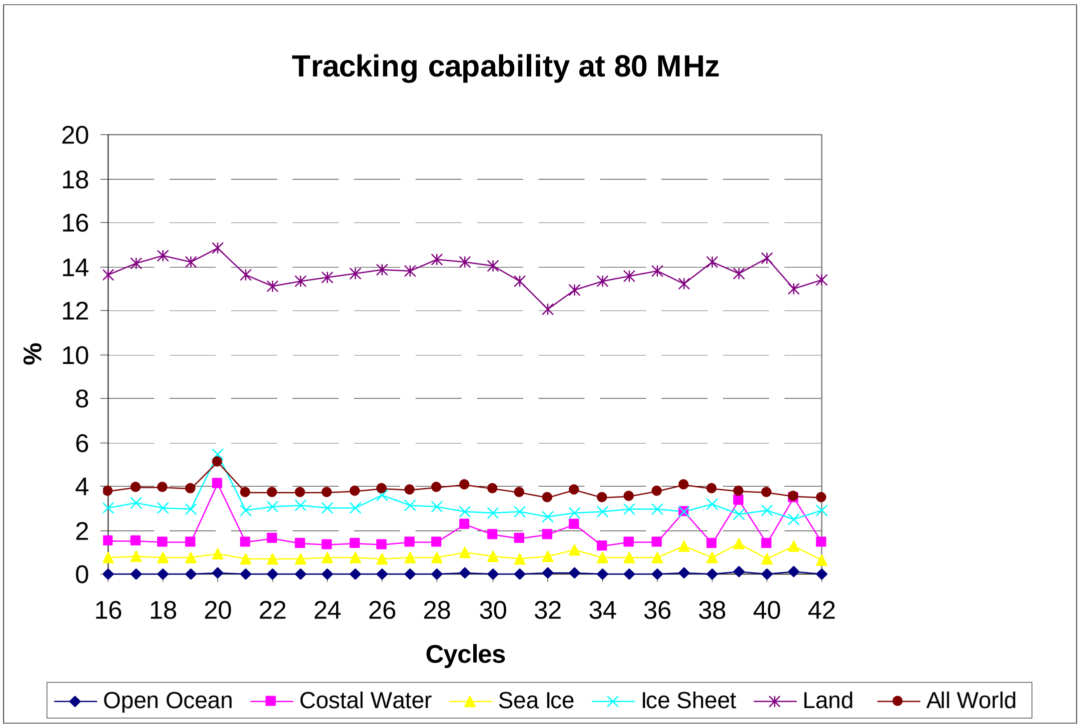

Figure 3: RA-2 Tracking percentage at 80MHz for different surfaces

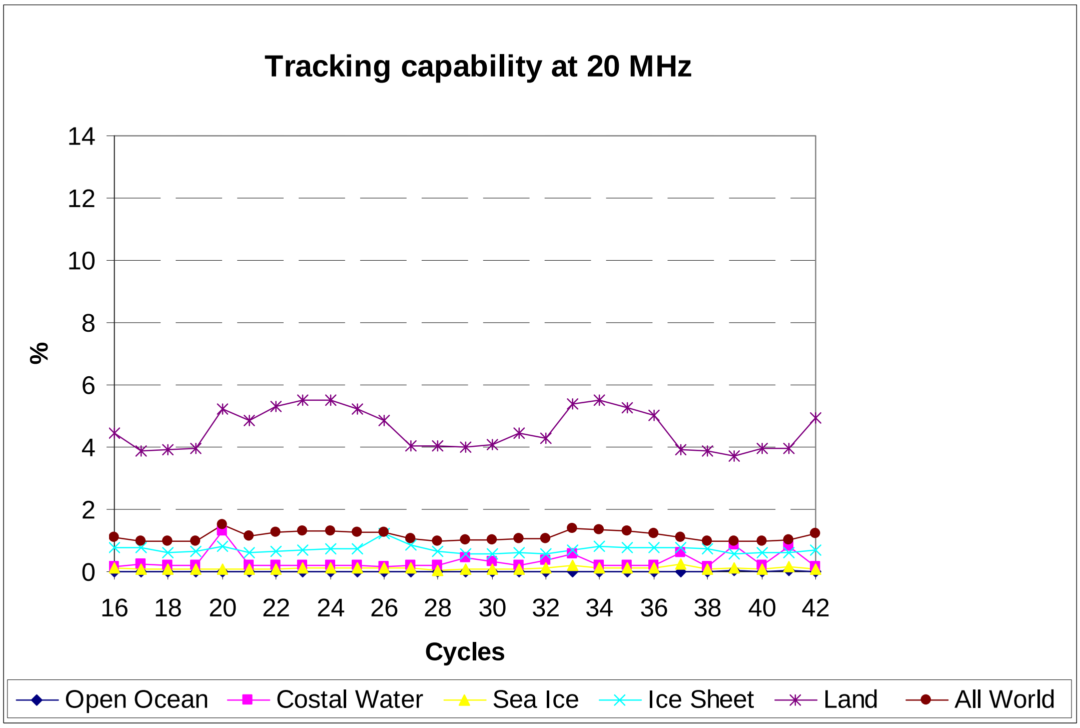

Figure 4: RA-2 Tracking percentage at 20MHz for different surfaces

6.1.2 IF FILTER MASK

In Figure 5 all valid IF masks retrieved by averaging the 100 seconds of data acquired daily during cycle 42 are plotted in the left panel. The on-ground measured IF mask (ref [R – 4]) is also plotted in that panel with a solid line. In the right panel, the difference of each of the calculated IF masks with respect to the on-ground measured one is reported. The average difference with respect to the on-ground is used as the criteria for defining valid masks: if it is lower than 0.01 dbs, the mask is considered valid. During cycle 42, the number of valid IF masks has been 19, representing about the 27% of the planned IF masks (70 per cycle). Only valid IF masks are used to generate the final IF mask used in the Level 1B ground processing; the method used for editing the data is based on the comparison between each of the single IF masks and the reference one (on-ground).

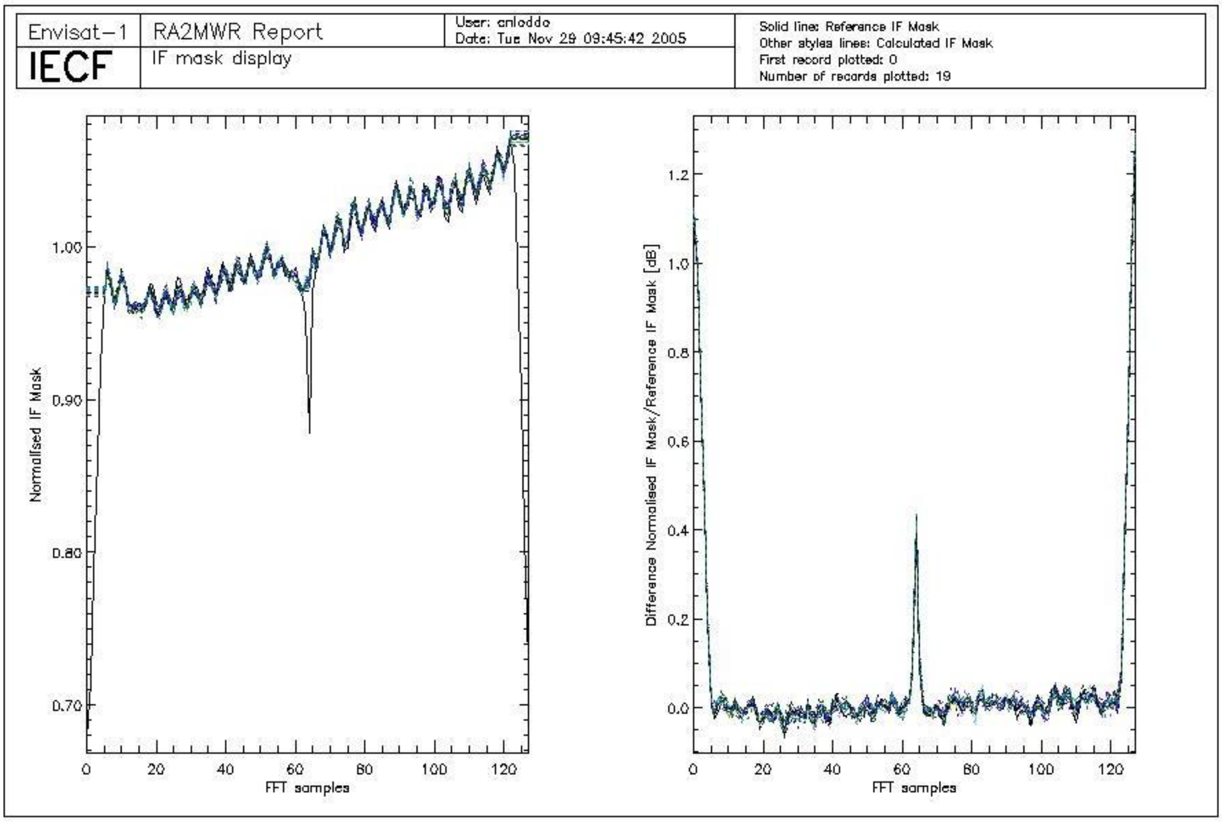

Figure 5: Valid IF masks retrieved daily during cycle 42 plotted together with the on-ground reference.

Since the 24th of October, the auxiliary file RA2_IFF_AX will be updated regularly once per month. In Figure 6 the on-ground measured IF mask is plotted with a solid line, the new IF Mask, updated on the 17th of November, and the previous IF Mask used for processing are plotted in dashed line.

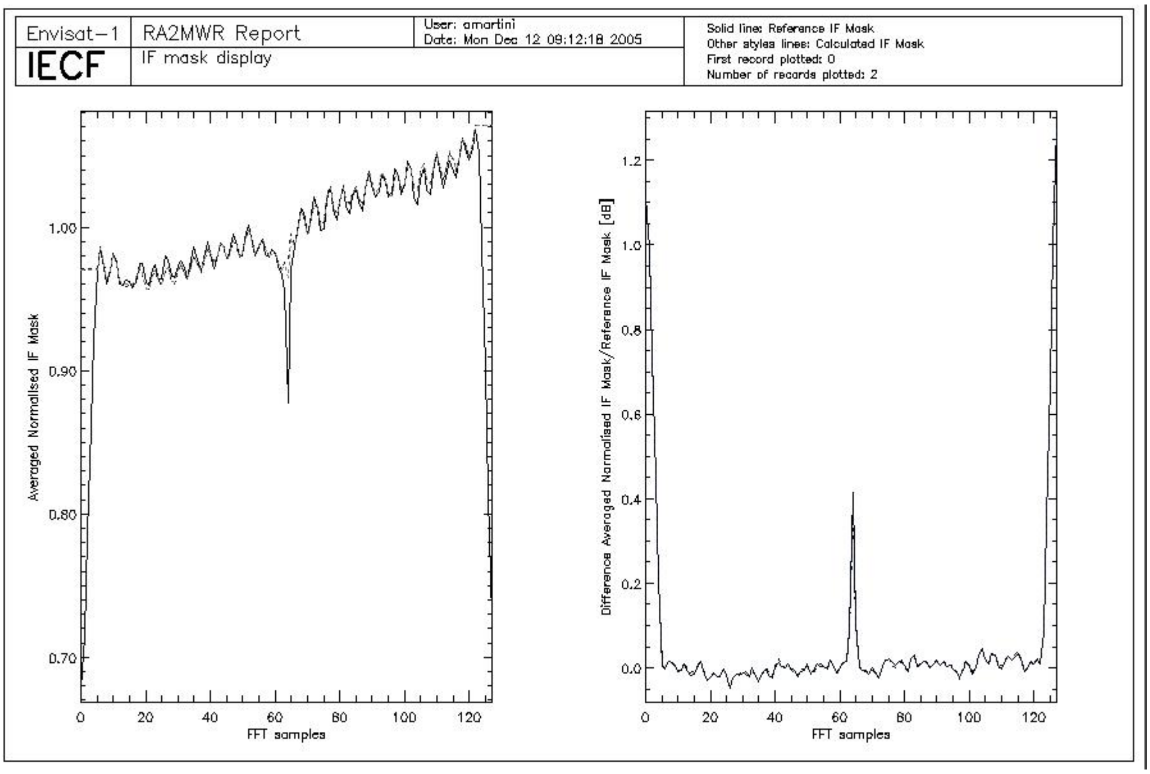

Figure 6: Previous and New IF Mask

In Figure 7 the evolution of the IF mask quality parameters evaluated as in [R – 4] is reported only for valid data. It can be observed that the difference with respect to the on-ground reference stays quite constant around 0.07 dBs.

Three peaks are visible on the plot that correspond to the data acquired on September the 27th 2003 at 15:48, on October the 29th 2003 at 15:42 and on May the 10th 2004 at 15:45. The reason of this could be found in the instrument warming up considering that the IF Cal acquisition has been made, in all the cases, only a couple of hours after an anomaly recovery. The residual noise and the accuracy show a very constant behavior over the whole period.

During cycle 42 the IF Calibration Mode still shows the weird behavior described in [R – 3]. This problem, present since the beginning of the mission, is under investigation. The anomaly directly affects the number of valid RA-2 IF masks obtained per cycle, but does not prevent the generation of the IF mask correction file, used in input to the Level 1B ground processing.

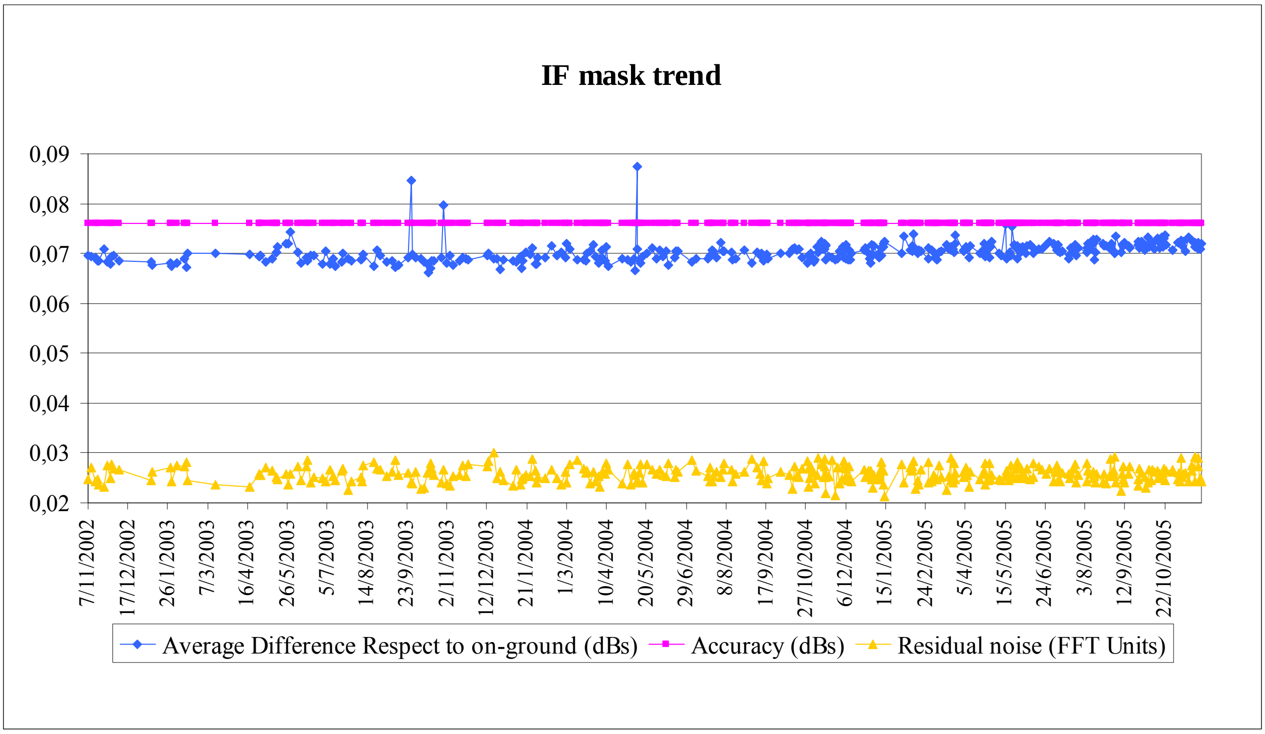

Figure 7: Evolution of the IF mask related parameters for valid IF masks retrieved up to cycle 42

In Figure 8 the percentages of valid IF masks from cycle 20 up to cycle 42 are reported.

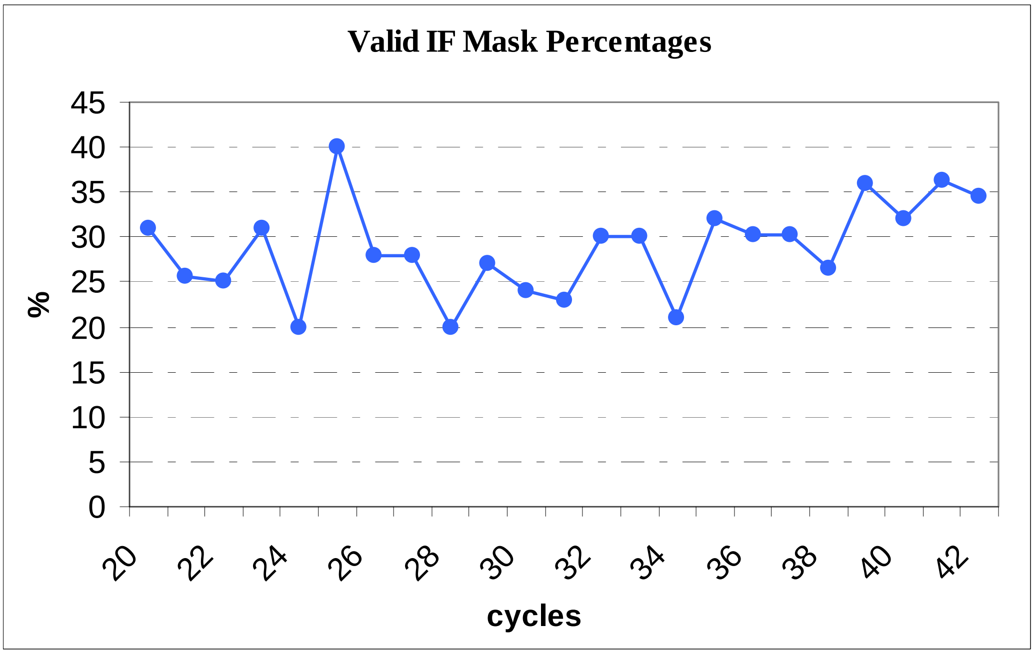

Figure 8: Percentages of valid IF Mask up to cycle 42

6.1.3 USO

Since the 24th of October, with the new IPF V5.02, the actual value of the USO clock period has been used within the L1b processing; this means that the data are corrected for the bias and the drift correlated to the actual USO clock period.
The evaluation of the actual USO clock period is performed off-line respect to the IPF processing and it is updated once per week in the auxiliary file RA2_USO_AX.
In Figure 9, the USO clock period trend retrieved for cycle 42 is reported. In order to make the variability visible, the difference of the actual USO clock period with respect to the nominal one has been plotted in the upper panel. In the lower panel the Range error due to the USO clock variability has been reported taking a satellite altitude of 800 Km as a nominal value.
The unusual behaviour of the USO clock period observed around the 3rd of November is related to some problems encountered in the UTC datation (Figure 11). Given that the algorithm used for the USO clock period evaluation is done using the UTC, this problem was reflected in the USO clock period computation. The problem was not reflected in the products given that the auxiliary file RA2_USO_AX has not been updated during this week.

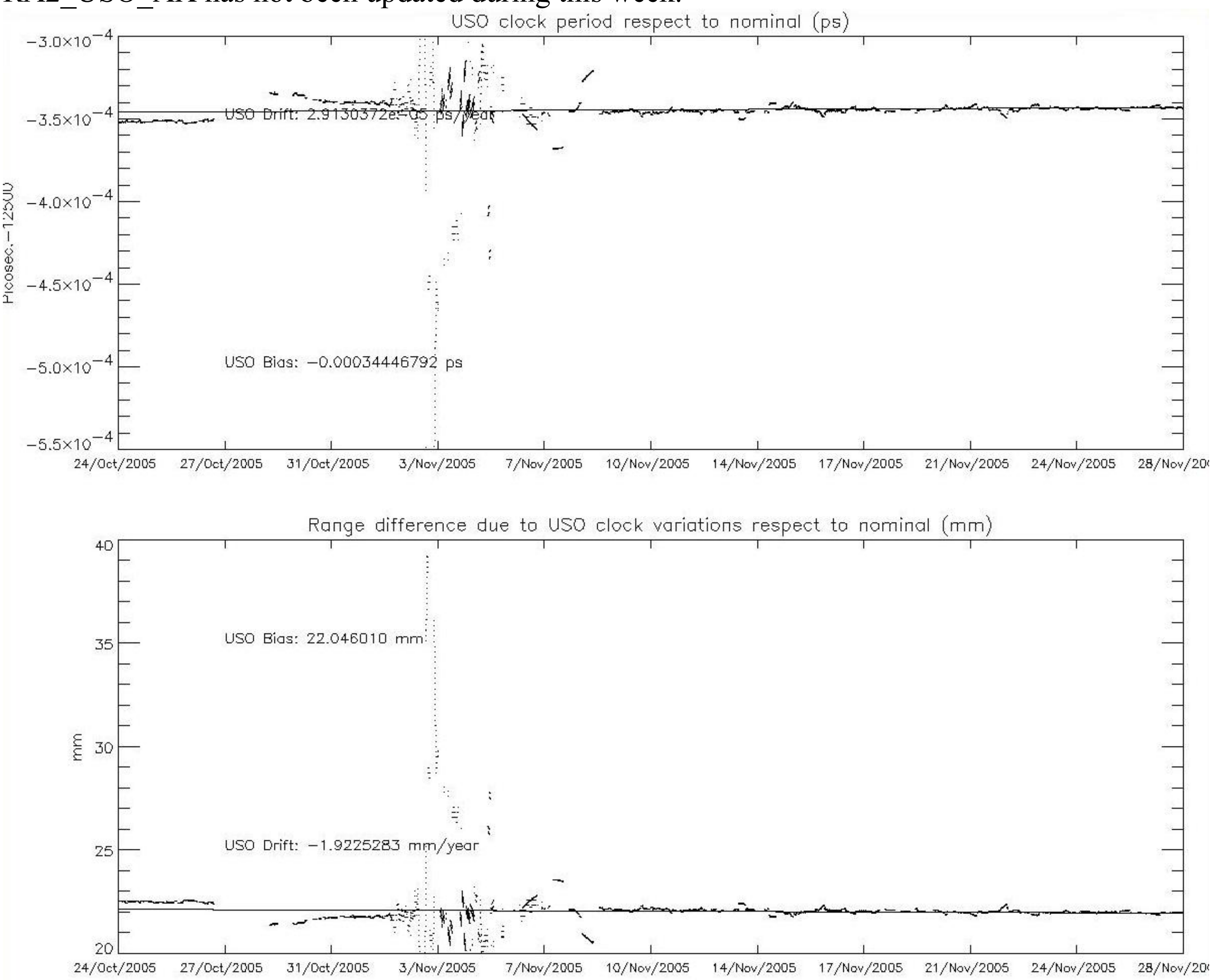

Figure 9: USO clock period for cycle 42

In Figure 10, the USO clock period trend retrieved until the end of cycle 42 is reported.
Given that the actual value of the USO clock period is used within the processing, the data are corrected for the bias and the drift correlated to the actual USO clock period. Those values, translated into altimetric range figures, are respectively of 29.4 mm and –4.6 mm/year as calculated with data covering the period 4 August 2004 to 19 September 2005 (the data covering the anomalous period between 2004/09/27 at ~16:00 and 2004/09/29 at ~12:00 AM have not been used to evaluate these figures).

WARNING: From cycle 42 onwards, users must not apply anymore the correction provided by ESA (Ref http://earth.esa.int/pcs/envisat/ra2/auxdata/).

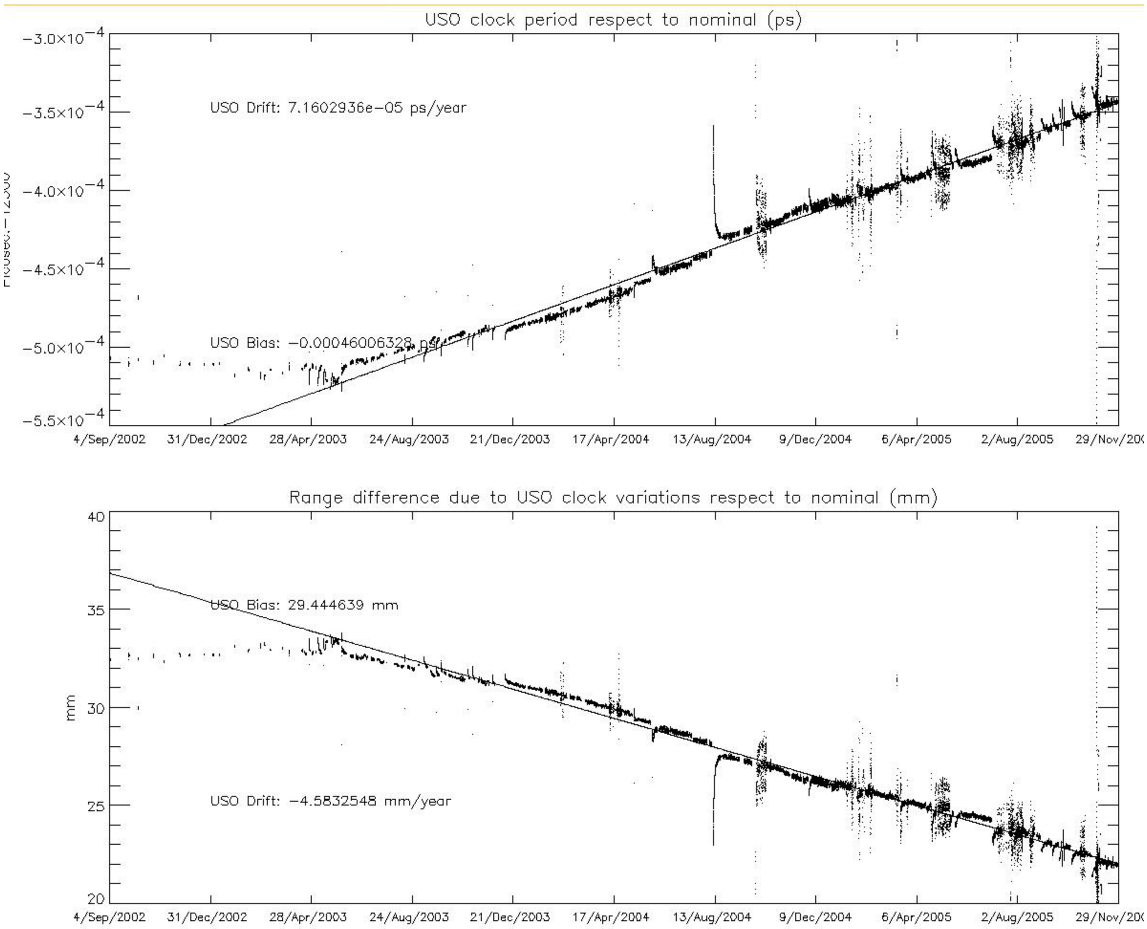

Figure 10: USO clock period until end of cycle 42

6.1.4 DATATION

A significant part of an eventual error in the RA-2 products datation could result from imperfect synchronisation between the Satellite Binary Time and the UTC Time due to a drift of the ICU clock period. A correlation between those two times is performed at every Kiruna orbit dump and then extrapolated for the four non-Kiruna orbits. In the upper panel of Figure 10, the differences between the extrapolated UTC values and the corresponding real UTC values measured at the next Kiruna dump, are reported.

In the lower panel, the ICU clock step for the same period is shown.

An anomalous event was observed around the 3rd of November, mjd 2133, Figure 11. For several orbits a sudden increase of the on-board USO step length affected the generation and the quality of a few Precise Time Correlation products. The expected and measured UTCs differ by more than 20μs, the threshold for assuming it as a good measurement. The problem lasted for about 3 days from the 3rd until the 7th of November.

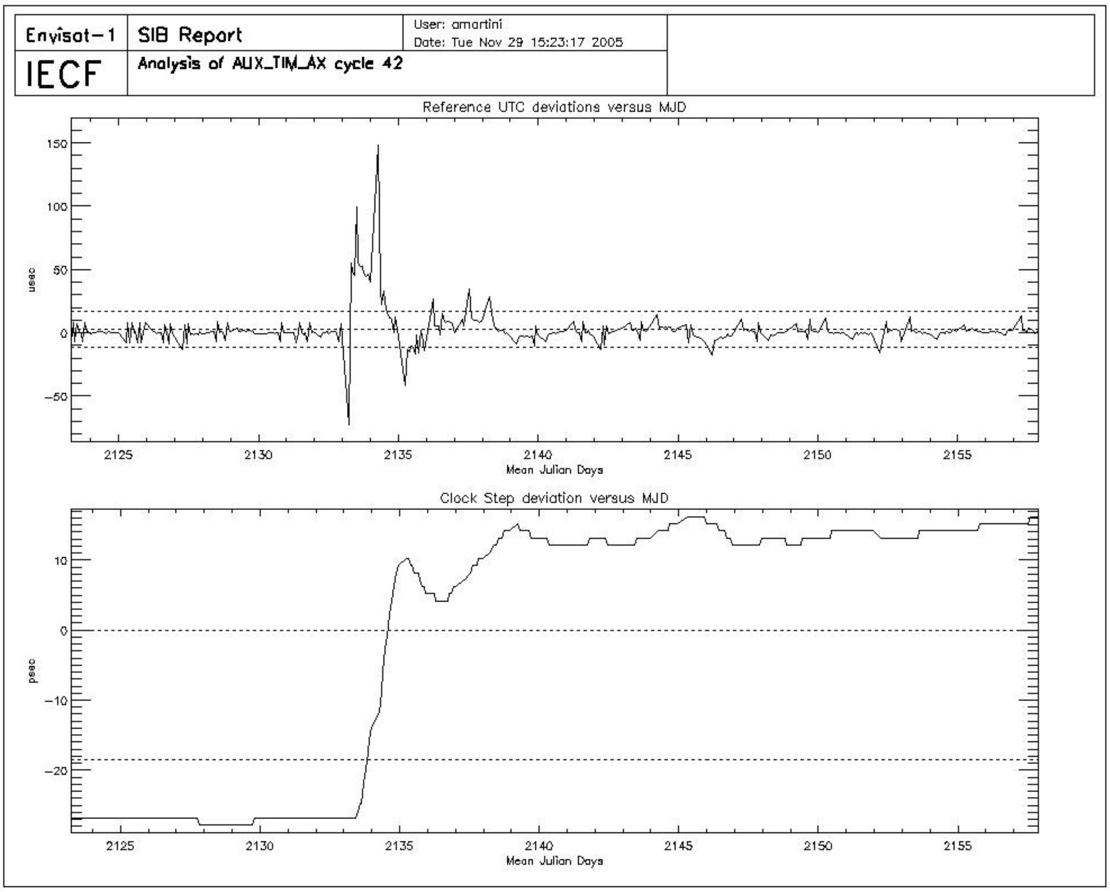

Figure 11: UTC deviations and ICU clock period for cycle 42

In Figure 12 (upper panel) the differences between the extrapolated UTC values and the corresponding real UTC values measured at the next Kiruna dump, are reported for data up to cycle 32. The UTC deviations for cycle 33 up to cycle 42 are reported in Figure 13.

Only a few anomalous events can be observed at the beginning of the period (cycles 16/17) for which the difference rises above the 20 microseconds warning threshold. However, starting from cycles 22/23, the number of small differences (10 microseconds plus or minus) has increased a lot. Furthermore, during the last ten days of the cycle 32 and for all cycle 33 and 34, the variability of the deviations has increased reporting many peaks just over the 20 microseconds threshold (first part of Figure 12); this phenomenon is now fixed. In the lower panel of both figures the ICU clock step for the same period is shown where big variations are reported. This is however not a problem because the ICU clock period variations are included in the algorithm for the SBT/UTC correlation evaluation.

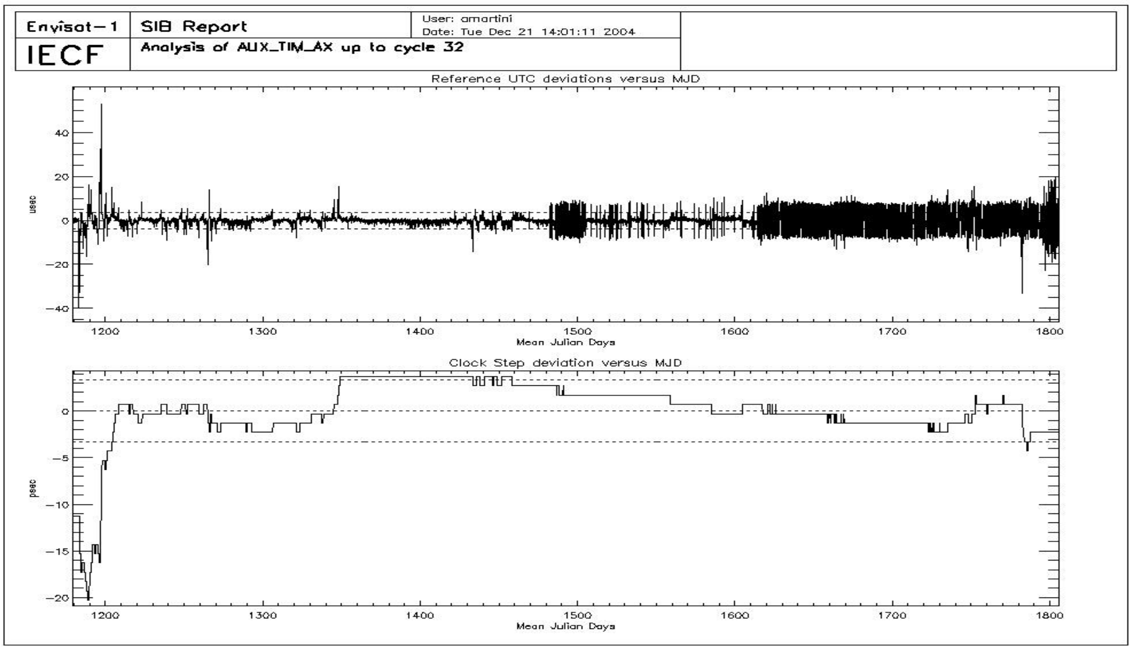

Figure 12: UTC deviations and ICU clock period up to cycle 32

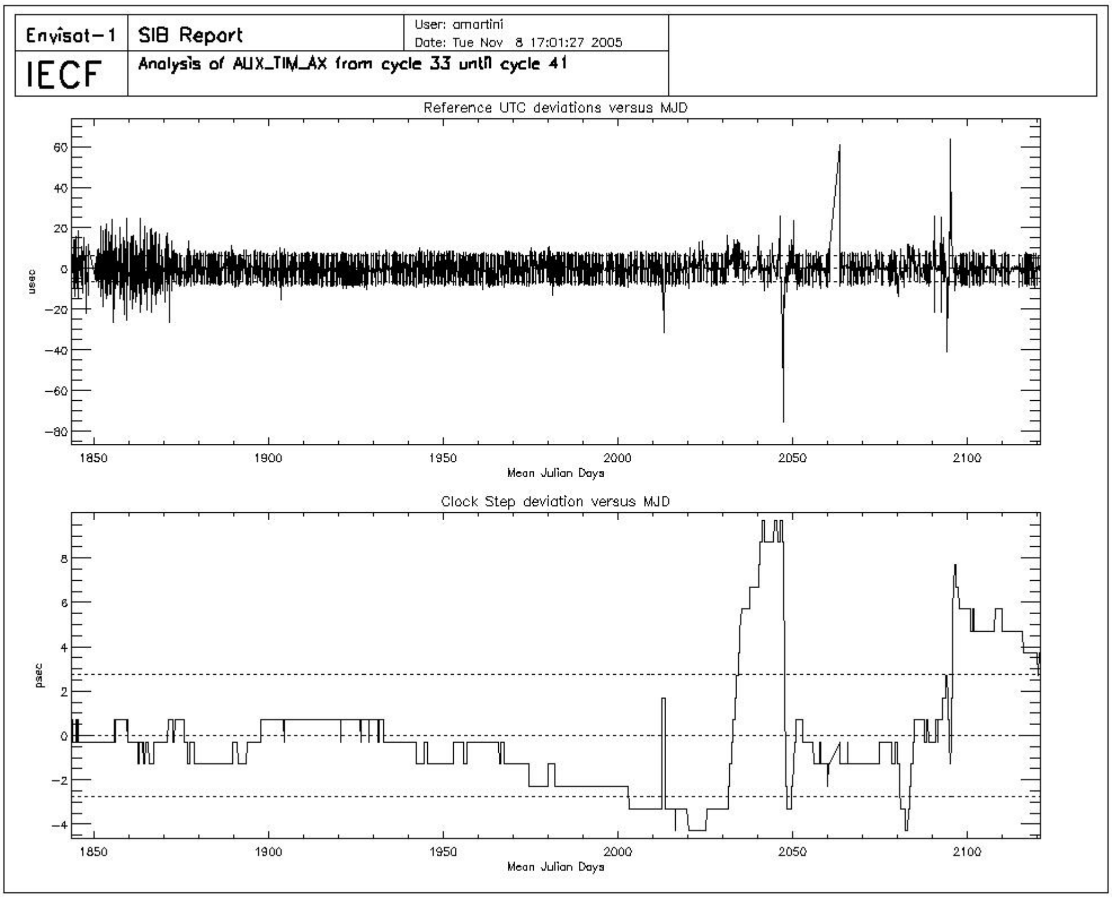

Figure 13: UTC deviations and ICU clock period from cycle 33 up to cycle 42

6.1.5 IN-FLIGHT INTERNAL CALIBRATION

The RA-2 Range and Sigma0 measurements are corrected to take into account the internal path delay and attenuation, respectively. This is done by measuring those two variables in relation to the internal Point Target Response. The two correction factors are calculated during the L1b processing and directly applied. They are also continuously monitored and the results for cycle 42 (averaged per day) are reported in the next figures. The high value of the Sigma0 calibration factor plotted in Figure 15 is related to the RA-2 anomaly recovery (see section 5.2.1). The Time delay in-flight calibration factor shows a regular behaviour as observed on previous cycles. The Sigma0 in-flight calibration factor shows a pronounced drift as in the previous cycle, decreasing from 0.38db to 0.33db.

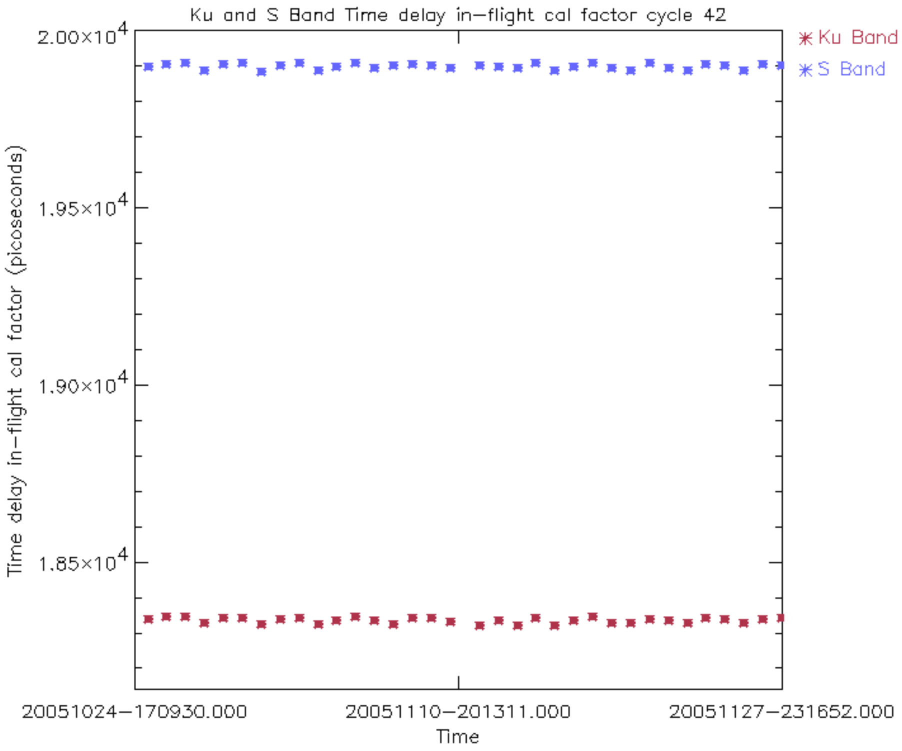

Figure 14: Ku and S Band in-flight time delay calibration factor for cycle 42

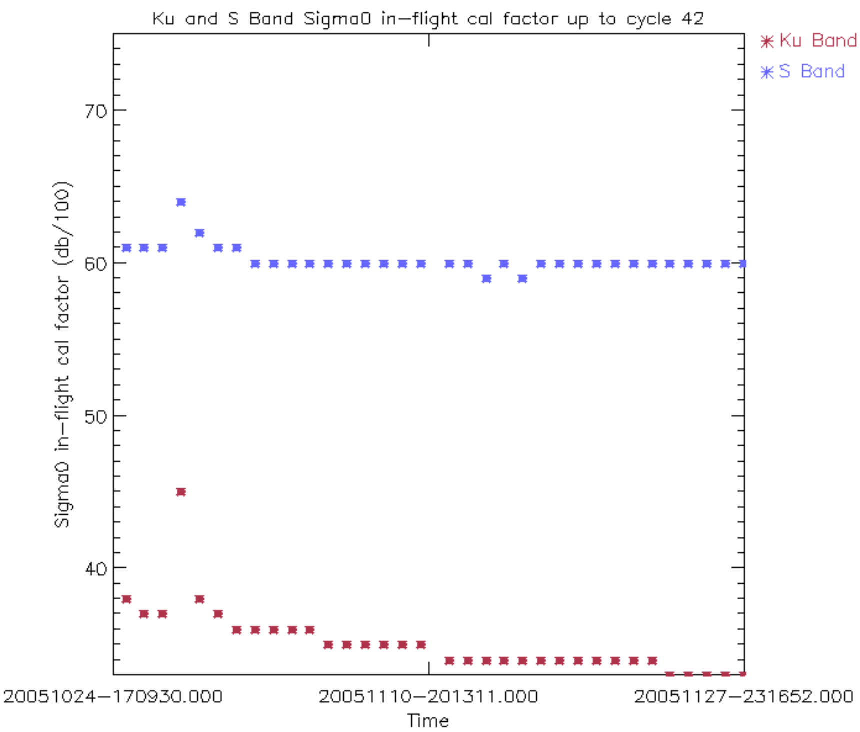

Figure 15: Ku and S Band in-flight Sigma0 calibration factor for cycle 42

Figure 16 and Figure 17 report Ku and S Band in-flight calibration factors for Time Delay and Sigma0 respectively, daily averaged, up to the current cycle. The Time Delay factor is shown to be very stable for both the working frequencies. The Ku band Sigma0 factor reveals a decrease of about 0.2 dBs over the period starting from cycle 16. As this instability is quite small, it is not being considered a problem for the moment, since the calibration factor is indeed introduced especially to correct for eventual instrumental changes. However, special attention is kept on the monitoring of this parameter.

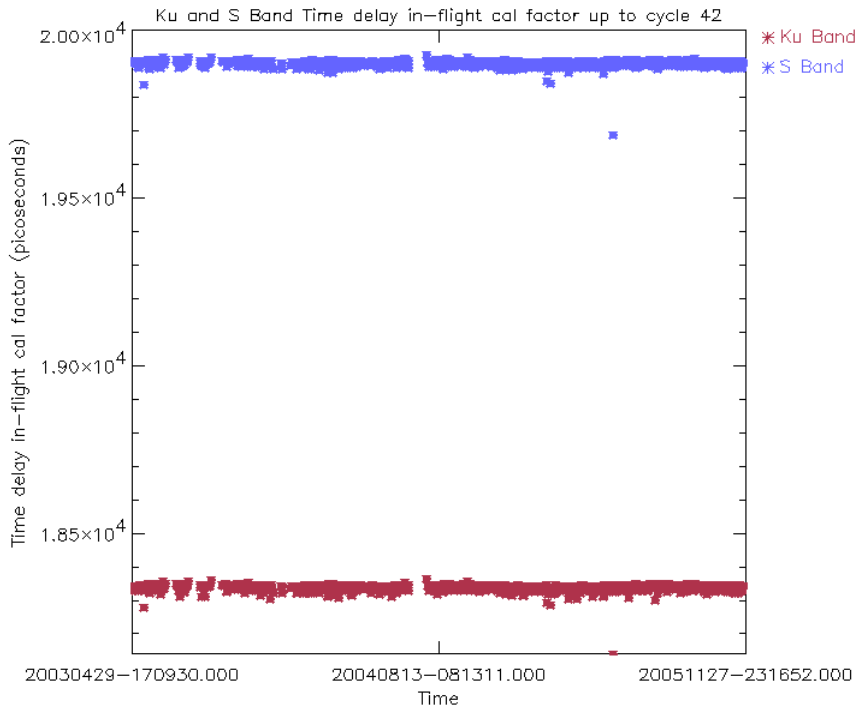

Figure 16: Ku and S Band in-flight time delay calibration factor up to cycle 42

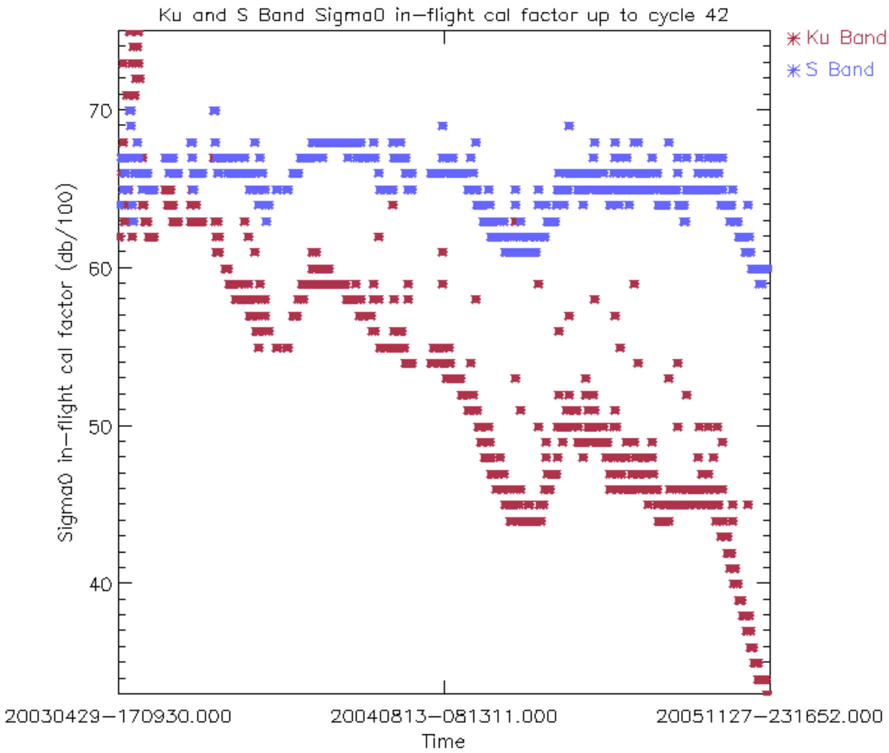

Figure 17: Ku and S Band in-flight Sigma0 calibration factor up to cycle 42

6.1.6 SIGMA0 TRANSPONDER

The σ° absolute calibration of the RA-2 is performed using a reference target given by a transponder that has been developed at ESTEC. This has been exploited during the 6 month Commissioning phase to generate early calibration results. In order to consolidate the calibration results and to monitor the RA-2 calibration of σ° during the Envisat lifetime, a continuous monitoring is needed by operating the transponder as many as possible Envisat overpasses.
Since the 11th of October the transponder has been moved to a permanent site located in Rome.
The results are reported in the following Table, including the tropospheric attenuation estimated from ECMWF data.

Orbit	Date	Location/Rel. Track	Coordinates	Resolution	Not Corrected Backscattering Bias [dB]	Tropospheric Correction (one way) [dB]
19407	15-Nov-05 20:39:21	Permanent site Rome / 315	42.8719, 12.4731	High	1.09	0.095

Table 2: Absolute backscattering calibration results obtained with Transponder measurements

Appendix 4 reports the transponder measurements from cycle 24 up to cycle 42.
The mean value of the estimated bias at High Resolution is 0.98 dB with a standard deviation of 0.07 dB. It is possible to notice that the Low Resolution measurements are coherent among

themselves but there is a bias with respect to the High Resolution ones. This is due to a processing problem with the internal calibration factor not taken into account in Low Resolution Mode.

In Figure 18, the time behavior of the bias is plotted for both Low and High Resolution. The green line represents the corrected bias for the internal calibration factor (only for the Low Resolution data) and the tropospheric attenuation. The latter is estimated by using the ECMWF meteorological data. The low value of the corrected bias for the orbit 14397 is due to the dew air condition and a probable underestimation of the tropo-attenuation.

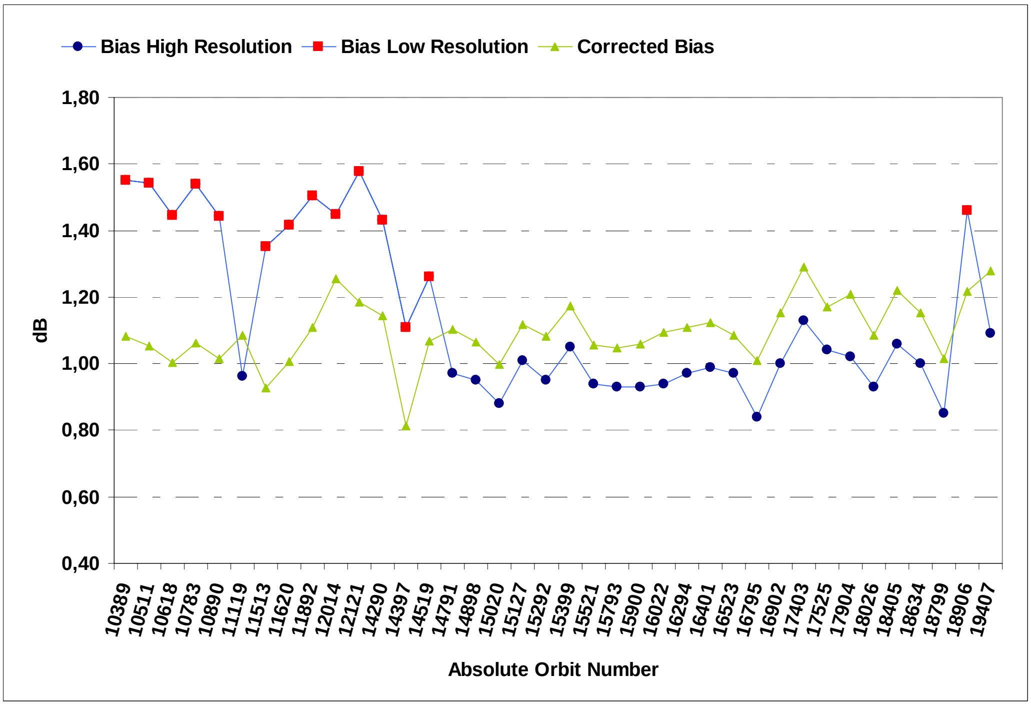

Figure 18: Time behavior of the transponder bias

6.1.7 MISPOINTING

In Figure 18, the trend of the mispointing squared (averaged every orbit) is reported in deg^2*10e-4.

The average squared mispointing value, as extracted from the RA2_FGD_2P data products, has decreased from about 0.028 deg^2, to 0.0075 deg^2. This is due to the new algorithm currently used to retrieve the mispointing value from the RA-2 waveform data, see section 5.1.1.1.

With the new IPF version 5.02, the mispointing is estimated through the waveform trailing edge slope using an optimum and fixed gate and no longer an adaptive window as defined previously. This allows avoidance of the filter bump effect that leads to high values of the mispointing.

For this cycle, one event of low mispointing values is present and visible in the plot of Figure 19. This event corresponds to the instrument anomaly occurred on the 28th of October, as reported in section 5.2.1.

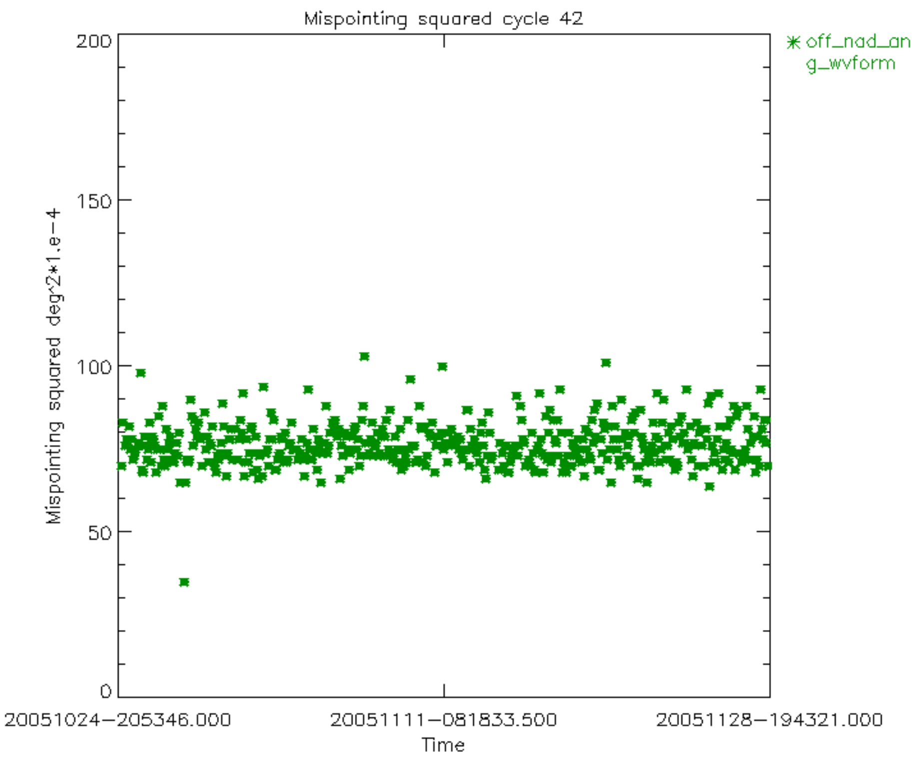

Figure 18: Smoothed mispointing squared trend for cycle 42 (deg^2*10^4)

In Figure 20, the overall mispointing squared trend (averaged over each orbit) is plotted for cycles 16 to 42.

The jump which occurred in the last part of the plot is related to the upload of IPF version 5.02, on date October 24th.. The abrupt decreasing of the mispointing squared value is related to the new algorithm, as described in the previous paragraph.

The jump which occurred on November the 26th 2003 is correlated to the upload of IPF version 4.56; the abrupt decrease of the mispointing squared value is due to the usage of a new RA2_IFF_AX IF mask auxiliary file. After the drop a very tiny increase of the mispointing squared could eventually be detectable. The most probable cause of this phenomenon could be a change in the Intermediate Frequency Filter slope due to ageing effects. For this reason, the RA2_IFF_AX will be updated regularly, once per month.

On the other hand, it can be noticed that the mispointing squared assumes lower values just after an instrument anomaly, showing an increasing trend until it reaches a standard mispointing value. This particular behavior can be explained by the different shape that the over-ocean average waveform has before and after an anomalous event as visible in Figure 21. Observe, in particular, the disappearance of the small dip in the waveforms acquired after the anomaly. This problem has been reduced with the introduction of the updated mispointing retrieval algorithm as described in the previous paragraph.

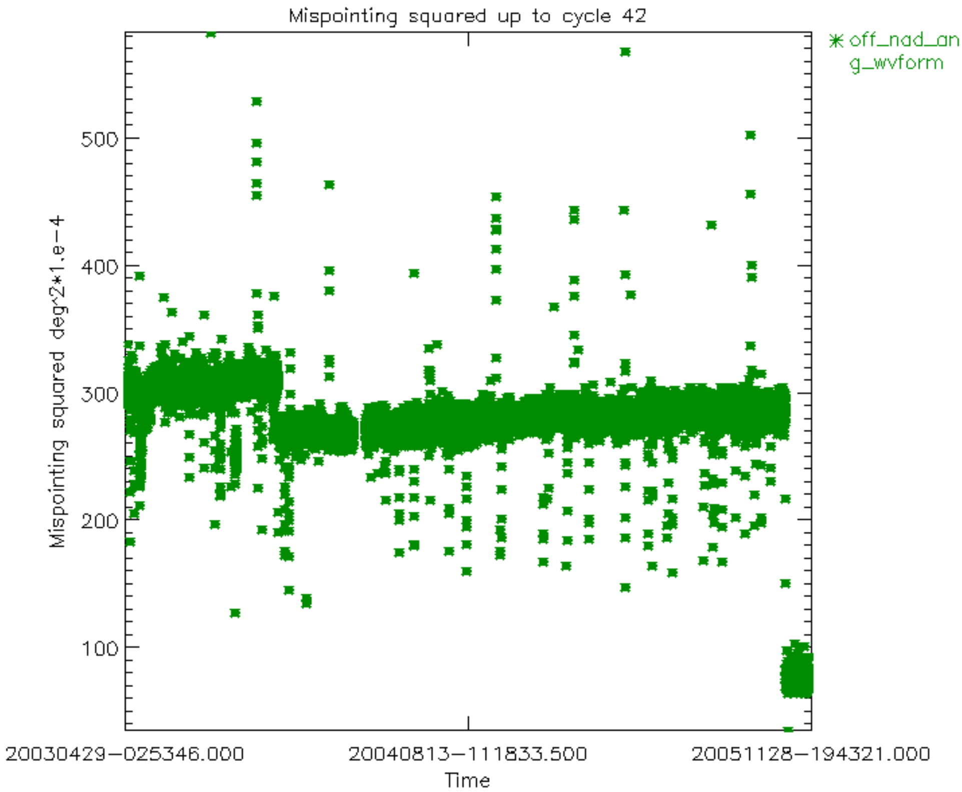

Figure 20: Smoothed mispointing squared trend until end of cycle 42 (deg^2*10e-4)

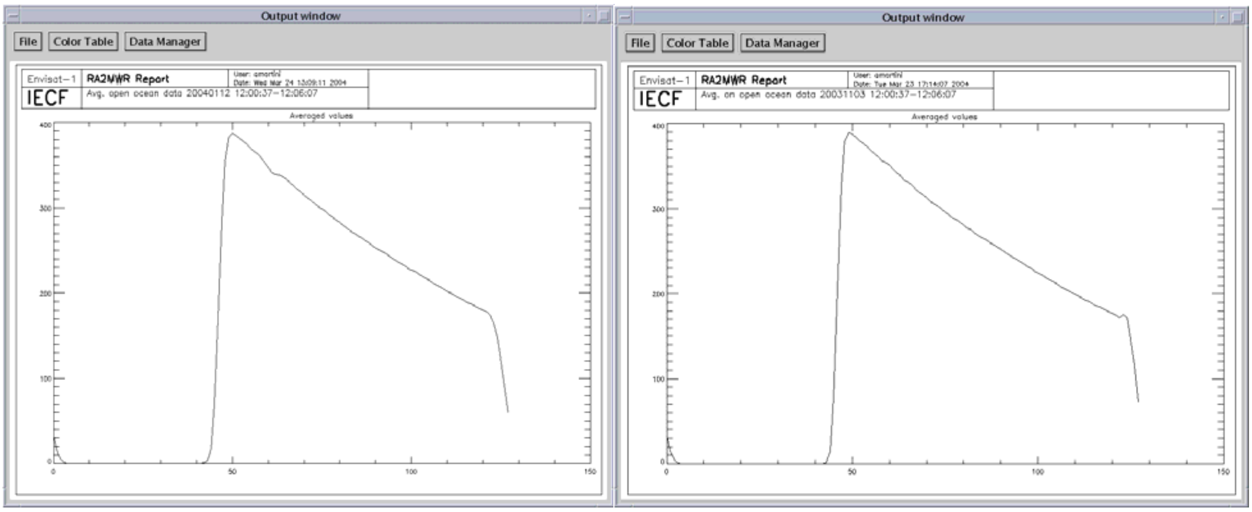

Figure 21: Open Ocean average waveforms before (left) and after an anomaly (right)

6.1.8 S-BAND ANOMALY

The so-called "S-Band anomaly" affects the RA-2 data products quality. Appendix 5 reports the list of the product files affected by the S-band anomaly problem during cycle 42. This corresponds to a total percentage of about 2.4% of the acquired data.

The method used for the identification of the "S-Band anomaly" is statistical and requires a minimum of 1000 seconds of data over ocean. This choice is supported by the fact that the "S-Band anomaly" is associated with a particular instrumental behavior that cannot appear and disappear within a short time frame. (ref. [R – 7])
A valuable algorithm to detect the RA-2 DSRs affected by the S-Band anomaly within the L2 products can be found in [R- 12]. Note that the algorithm is only valid for data acquired over open-ocean.
The IPF version 5.02 includes an algorithm that can detect the presence of the so-called "S-Band anomaly" over any surface. In case of S-Band anomaly detection, bit 1 of the L1b products MCD is set to one; the anomaly is properly detected in 99.9% of the cases. Due to several troubles encountered during the implementation of IPF version 5.02, the S-band anomaly detection flag (bit 1 of the RA-2 L1b MCD) cannot be trusted in this IPF version. As reported in chapter 5.5.1, this problem will be solved with the new release of the IPF, at the beginning of next year.

In Figure 22, the percentage of data per cycle that are affected by the so-called "S-Band" anomaly is reported. The figures are variable between 0% and 8.1%.
The number of occurrences of the S Band anomaly decreased from a mean value of 4% to 2% from cycle 31 until cycle 42 due to the implementation of the IF CAL procedure (including Heater 2 for S Band anomaly suppression) twice per day over the Himalayan region. However, this number increased during the last three cycles.
The relatively high value recorded for cycle 27 is due to the fact that on the day 1st of June 2004, the S-band anomaly started at around 14:30 while the instrument didn't switch to mode Heater 2 when foreseen (at about 15:50). For this reason the S-Band anomaly continued for the next 24 hours until the next Heater 2 mode on June the 2nd.

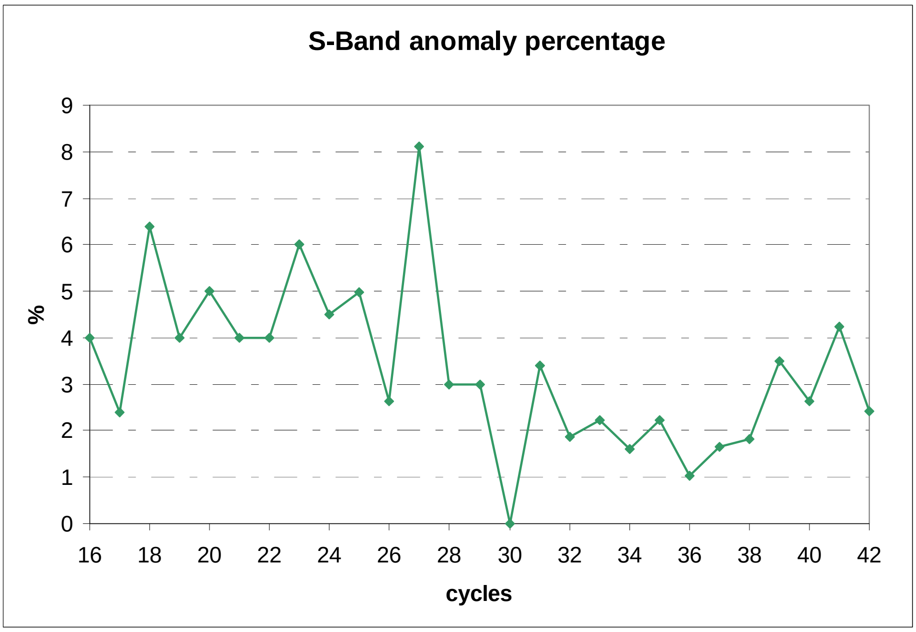

Figure 22: Percentage of data affected by the "S-Band Anomaly" for cycles 16-42

6.2 MWR Performance

For MWR performance please refer to the Reference CLS Cyclic Report of the type of [R – 2].

6.3 DORIS Performance

For DORIS performance refer to the Reference F-PAC Monthly Report of the type of [R – 1a] and [R-1b].

7 PRODUCT PERFORMANCE

7.1 Product disclaimer

A summary of the products released to users and disclaimers on product quality have been established for some products and are available in the following web link: http://envisat.esa.int/dataproducts/availability/

7.2 Data handling recommendations

7.2.1 SEA-ICE FLAG

The following algorithm is proposed for the determination of a sea-ice flag, presently missing in the Level 2 Ra-2 and MWR data products. (See [R – 14]):

|Latitude *(lat: field#4 of L2 data)*| >50 deg
AND
The number of 20Hz valid data *(num_18hz_ku_ocean: field#23 of L2 data)* < 17
OR
|MWR Wet Tropospheric Correction *(mwr_wet_tropo_corr: field#42 of L2 data)*–ECMWF Wet Tropospheric Correction *(mod_wet_tropo_corr: field#42 of L2 data)*| > 10 cm
OR
Peakiness *(Ku_peak: field#139 of L2 data)* >2

7.2.2 OCEAN S-BAND ANOMALIES DETECTION

A valuable algorithm to detect the Level 2 DSR affected by the RA-2 S-Band anomaly is proposed in [R- 12]. Note that its validity is limited to the data acquired over open-ocean.

7.2.3 WARNING ON IPF 4.56 VERSION IDENTIFICATION FIELD

All RA-2 and MWR level 1B and NRT Level 2 products generated after November 26, 2003 report a software version as being 4.54 (available in MPH field 8).

Nevertheless those products have been generated with the IPF V4.56 operational since November 26, 2003. The first nominal generated product, using the new SW version, will be the one relevant to the absolute orbit number 9094.
The software version ID is correct since December 4, 2003.

7.2.4 S-BAND BACKSCATTERING COEFFICIENT

For the data processed with IPF version 4.56 on, the S-Band Backscattering coefficient has been demonstrated to be on average about 0.65 dBs higher than for the previous versions of the processor. This is due to the algorithm used for the retrieval of the AGC in S-Band, corrected in IPF version 4.56 to be closer to the real functioning of the instrument.

An average value of 0.65 dBs is suggested to be added to the old software versions S-Band Sigma0 in order to be in line with the new IPF V4.56 version.

7.2.5 USO RANGE CORRECTION

The actual data of cycle 42 don't have to be corrected to compensate for the Ultra Stable Oscillator drift shown in Figure 9. As reported in chapter 6.1.3, since the 24th of October, with the new IPF V5.02, the actual value of the USO clock period has been used within the L1b processing.

Users are advised to not correct anymore the range with the correction provided by ESA (Ref http://earth.esa.int/pcs/envisat/ra2/auxdata/).

All data acquired before cycle 42 still have to be corrected. The measured Range shall be corrected considering a drift of -4.58 mm per year and a bias of 29.6 mm.

Warning for data acquired before cycle 42: bias and drift have to be **SUBTRACTED** from the original altimetric range, according to the following equation:

Rtrue=Roriginal-dR

where Roriginal is the range in the GDR products and Rtrue is the true (corrected) range.

7.2.6 KU-BAND BACKSCATTERING COEFFICIENT CALIBRATION

The results of the Ku-Band Sigma0 absolute calibration performed with a transponder have been presented in par. 6.1.4. Those results are going to be consolidated and are summarized in chapter 9.1.4. In order to absolutely calibrate the backscattering coefficient given in the RA2 L2 products, the following shall be used by the end user to get to the real Sigma0 measurement:

Sigma_0_true = Sigma_0_prod + G_tx_rx_prod - G_tx_rx_real - Bias [dB]

Where:
Bias: Bias retrieved from the Sigma0 Absolute Calibration (see 9.1.4)
G_tx_rx_prod: Current effective Tx-Rx Gain value used in the operational ground processing chain (ADF file RA2_CHD_AX). The value nominally used since IPF V4.54 is (for configuration RFSS=A and HPA=A) is 170.70 dB
G_tx_rx_real: Pre-launch characterization value (configuration value RFSS=A and HPA=A is 167.46 dB)

7.2.7 ABNORMAL RA-2 RANGE BEHAVIOR AFTER ANOMALY RECOVERY

An un-expected behavior of the Envisat RA-2 sensor was observed in the period from 2004/09/27 at ~16:00 and ending on 2004/09/29 at ~12:00 AM. This directly happened after the recovery of a RA-2 on-board anomaly occurred on the 2004/09/26 at ~13:40. The altimetric range jumped by several meters w.r.t. the Mean Sea Surface; on the other hand everything came back to normal as from the 29th of September around noon. RA-2 data from the above period have to be considered with caution.

7.3 Availability of data

7.3.1 RA-2

In Figure 23 and Table 9 (Appendix 2) the summary of unavailable RA-2 L0 products is given.
It is easy to notice that close to the Himalayan region two small gaps in the data are present. This is due to the daily instrument switch-offs (Heater 2 mode) performed to prevent the S-Band anomaly lasting more than half a day if it occurs.

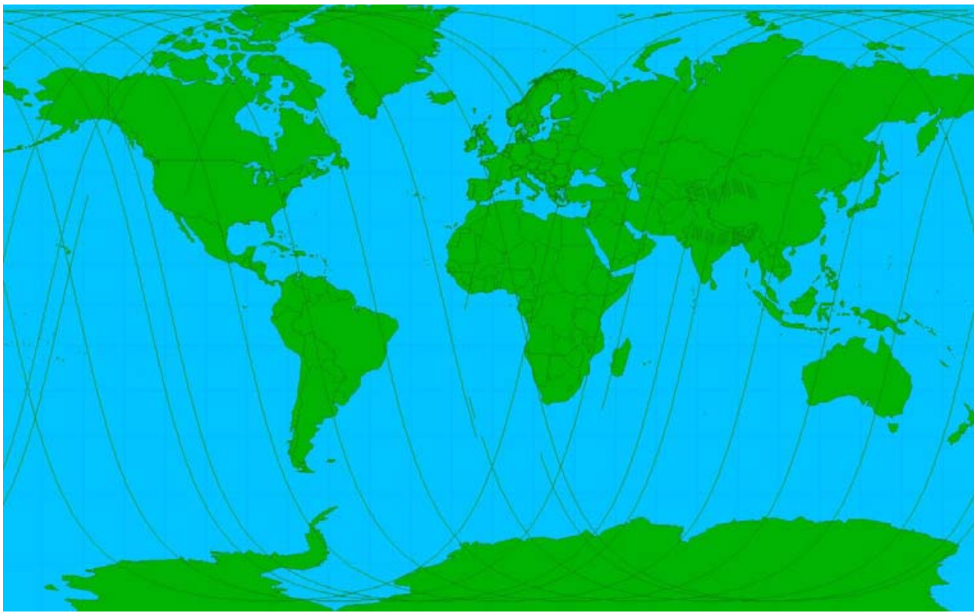

Figure 23: RA-2 L0 unavailable products for cycle 42

In Figure 24 and Table 11 (Appendix 2) the summary of unavailable RA-2 L1b products is given.

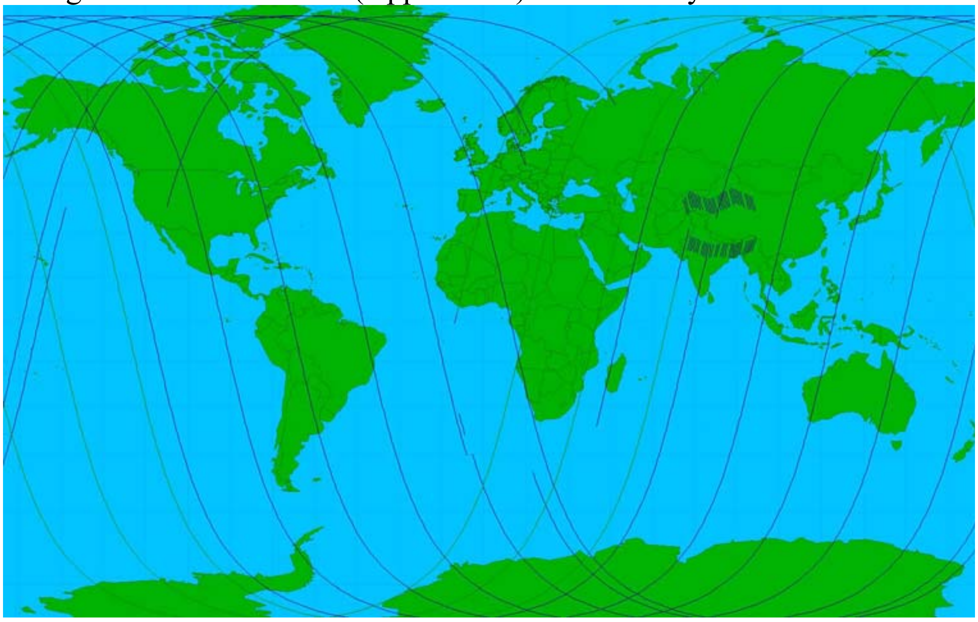

Figure 24: RA-2 L1b unavailable products for cycle 42

Hereafter the percentage of the different levels of products availability is reported. Considering as reference the instrument unavailability, it is possible to notice that since cycle 32 the situation is slightly improved for all levels of products.

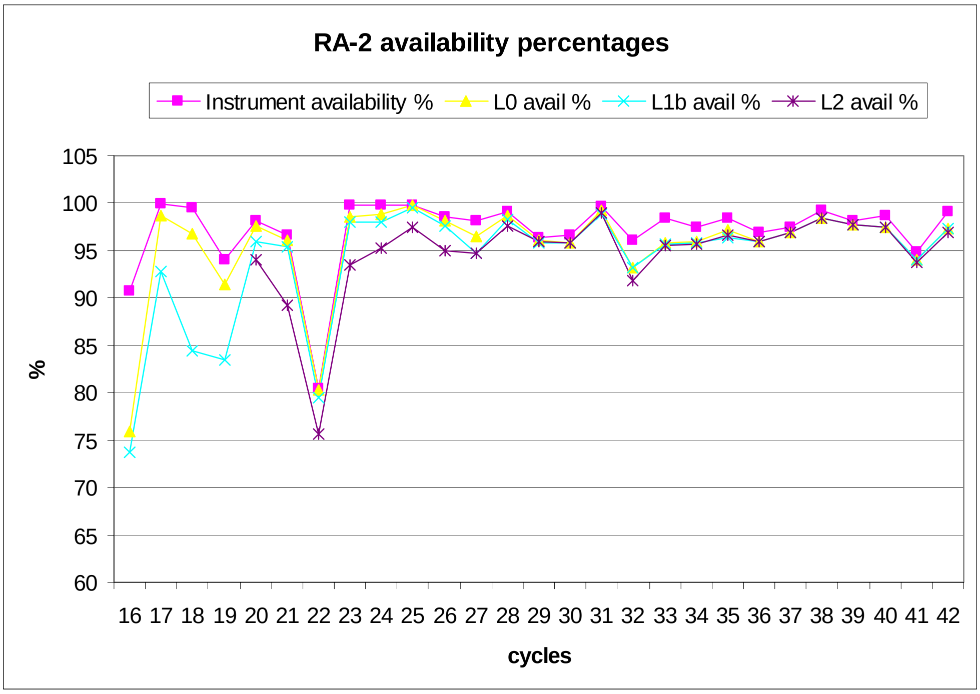

Figure 25: Percentage of Products unavailability up to cycle 42

7.3.2 MWR

In Figure 26 and Table 10 (Appendix 2) the summary of unavailable MWR L0 products is given.

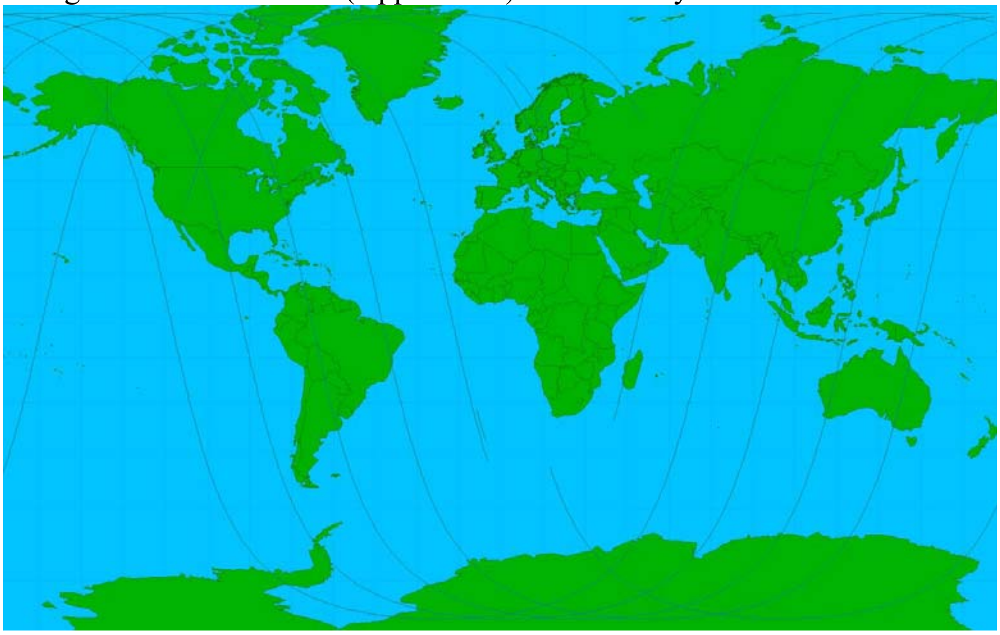

Figure 26: MWR L0 unavailable products for cycle 42

7.4 RA-2 Altimeter Parameters

Hereafter a summary of the main Altimetric parameters performances is reported; these results have been obtained using only ocean surface type and all world zone criteria for RA2_FGD products.

7.4.1 ALTIMETER RANGE

Since the 24th of October, operations date of IPF version 5.02, the DORIS Navigator data were expected to be used to evaluate the location, the altitude and the altitude rate corresponding to any Data Set Record of the products. However, due to some planning problems encountered, only the last part of cycle 42 has been processed using DORIS NRT orbital information computation.
The problem has been fixed and since the 21st of November, orbit number 19485, almost all NRT data have been processed using DORIS NRT orbital information computation.
The monitoring of the RA-2 FD altimetric range will not be done in this cycle given the small amount of NRT data processed using DORIS.

7.4.2 SIGNIFICANT WAVE HEIGHT

The histogram of the SWH reported in Figure 27, shows a nominal behavior for this cycle. The trend goes on following the behavior as detected for the previous cycle. The largest peak (about 60000 data for SWH = 0m) was removed from the plot in order to have the complete picture of the SWH histogram.
Figure 28 shows the SWH daily mean. The possible high values, plotted outside the figure range, reported for the S-Band data are due to the so-called S-Band anomaly (ref. par.6.1.8).

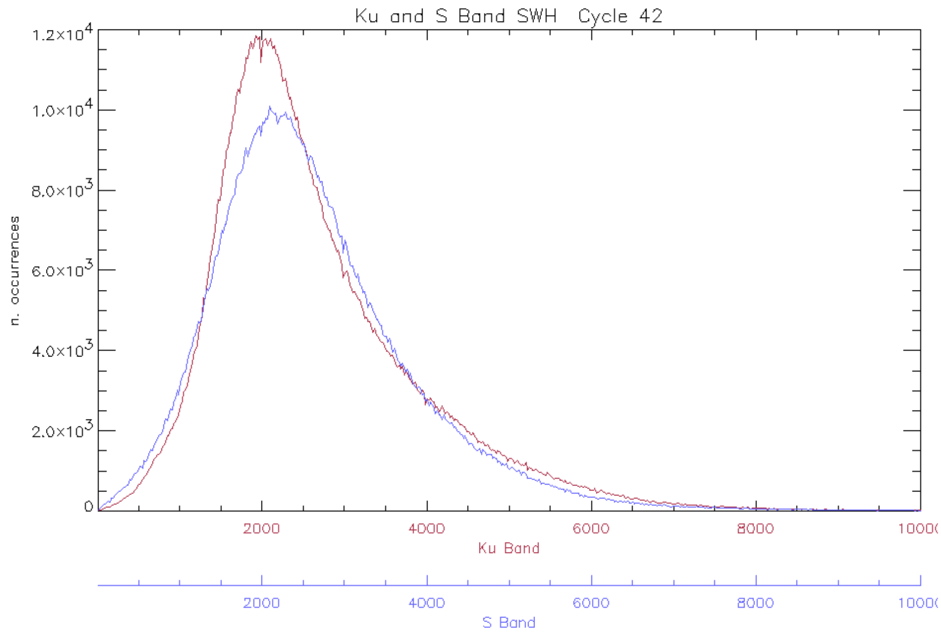

Figure 27: Histogram of Ku and S Band SWH for cycle 42 (mm)

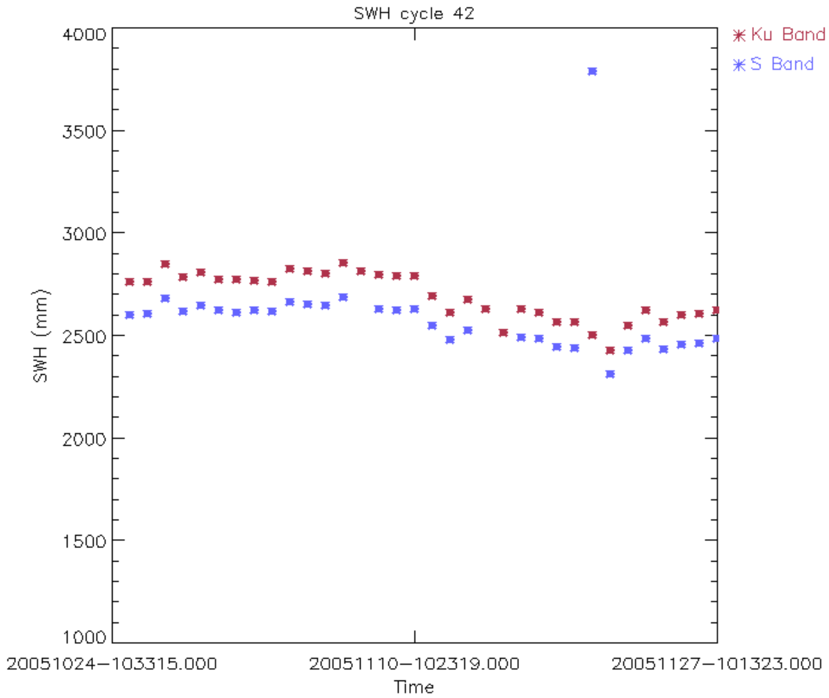

Figure 28: Ku and S SWH daily average for cycle 42 (mm)

In Figure 29, the SWH is reported from cycle 16 until cycle 42. It can be noticed that the SWH in both bands shows a trend which follows the seasonal variability. The high daily means reported (sometimes plotted outside the figure's range) are due to the so-called S-Band anomaly (ref. par.6.1.8).

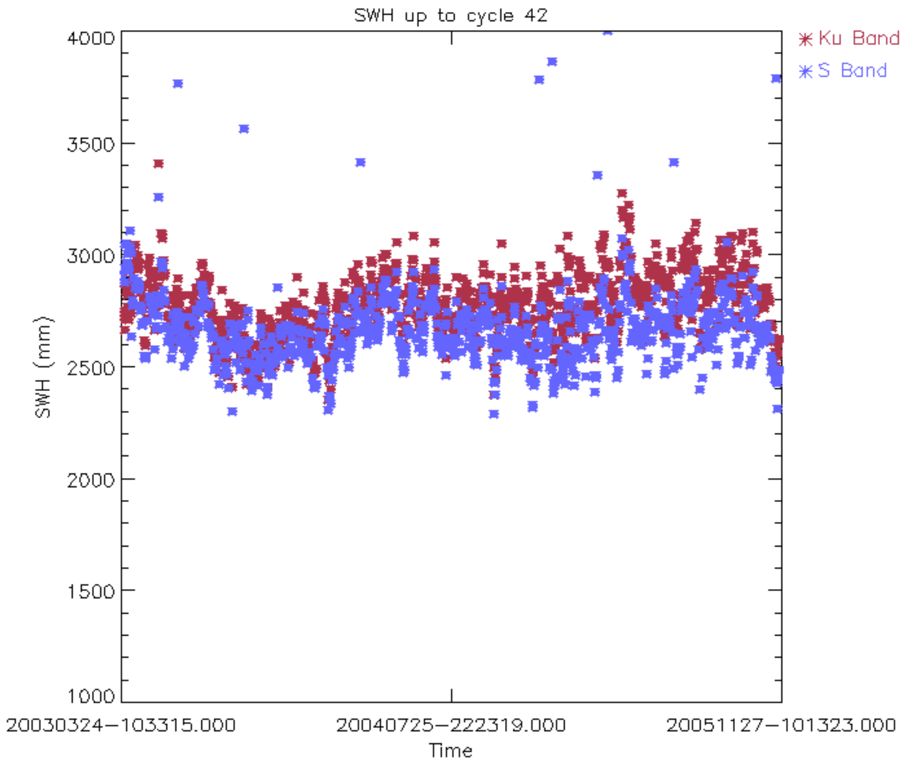

Figure 29: Ku and S SWH daily average up to cycle 42 (mm)

7.4.3 BACKSCATTER COEFFICIENT – WIND SPEED

The Sigma_0 histogram both in Ku and S Band, shows secondary peaks, see Figure 30. A small investigation on this problem, performed on the data of cycle 28, demonstrated that the backscattering distribution assumes a different behaviour for different sea conditions [R-17]. Indeed, for both bands, the majority of the data is concentrated on lower values for rough sea state (southern hemisphere, winter conditions) and on higher values for calm sea state (northern hemisphere, summer conditions).

In Figure 31, the backscattering coefficient daily average, computed for only ocean data, trend is reported. The trend shows a nominal behavior for both bands. The S-Band Sigma_0 daily means, that are plotted outside the figure range, can be traced back to the so-called S-Band anomaly (ref. par. 6.1.8).

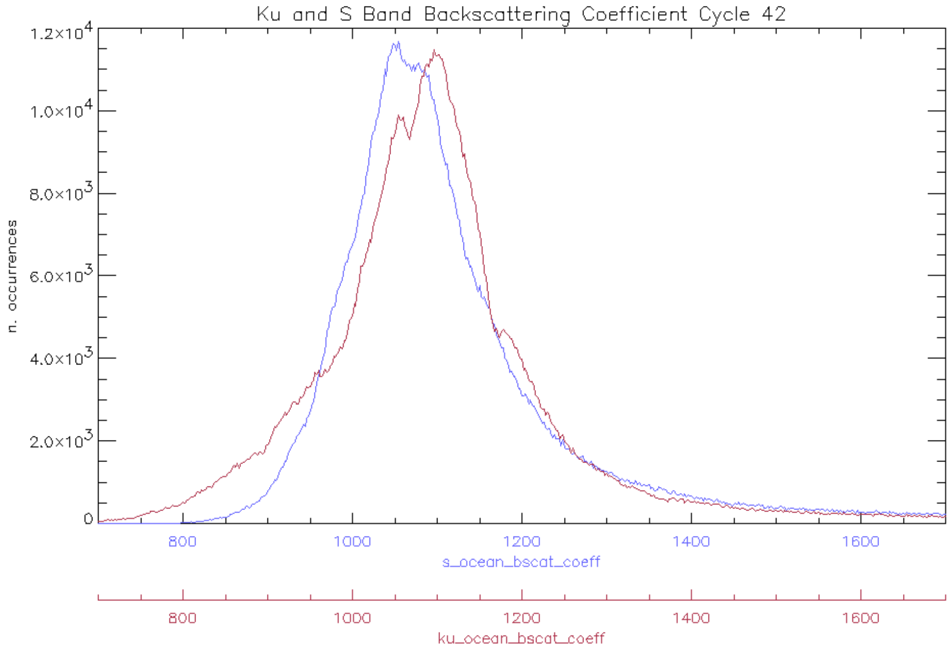

Figure 30: Histogram of Ku and S Band Backscattering Coefficient for cycle 42 (dB/100)

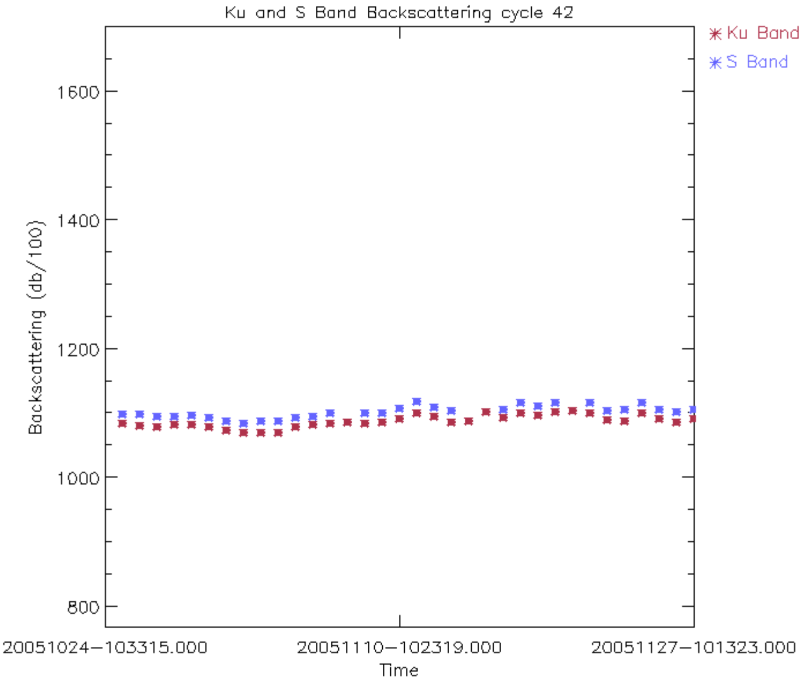

Figure 31: Ku and S Sigma_0 daily average for cycle 42 (dB/100)

The histogram of Wind Speed computed for the Ku-band and the time behavior during cycle 42 are reported in Figure 32 and Figure 33, respectively. Given that the wind table has been updated, P. Janssen Table is now used, the wind takes values between 1.18m/ and 21.30m/s.

The largest peak present in the histogram (about 50000 data for Wind < 1.2m/s) was removed from the plot in order to have the complete picture of the wind histogram.

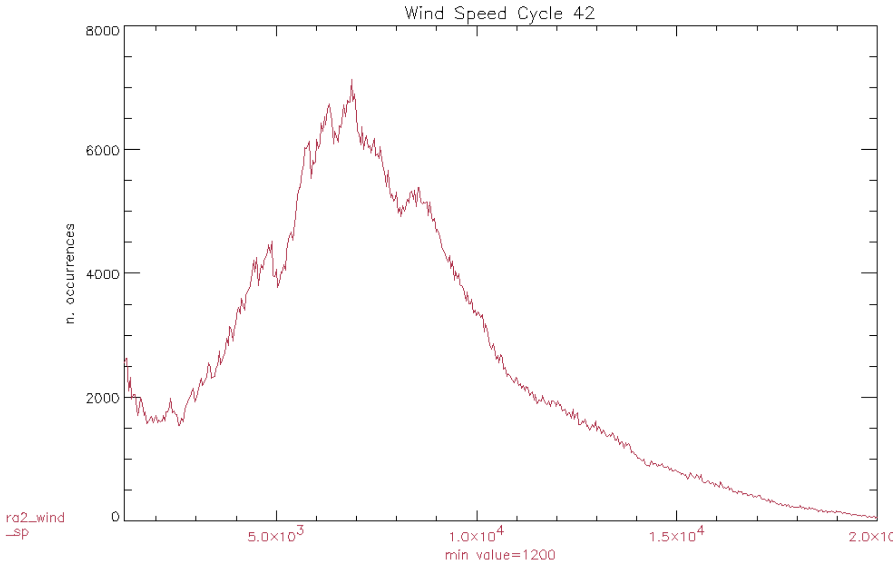

Figure 32: Histogram of Ku Wind Speed for cycle 42 (mm/s)

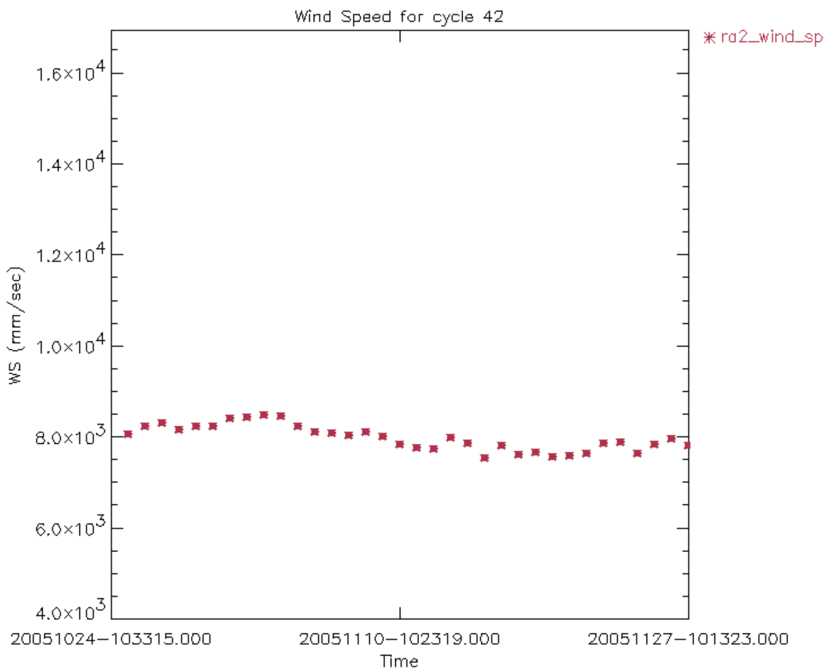

Figure 33: Ku Band Wind Speed daily average for cycle 42 (mm/s)

The Ku-Band Sigma_0 trend, reported hereafter, is characterized by a jump of on average 3.24 dBs concomitant with the operational up-load of IPF version 4.54 which occurred on the 9th of April 2003. This change is due to the upload of a new RA2_CHD_AX ADF file that artificially shifted

the RA-2 real Sigma_0 in order to align it with ERS-2 Sigma_0 and make it coherent with the Witter and Chelton empirical wind model. A similar change in trend, but in the opposite direction, is also visible in the Wind Speed trend reported in Figure 35.
Beyond the huge jump that occurred in April 2003, the S-Band Sigma_0 reports a smaller jump occurring on November the 26th 2003. Following the installation of the IPF processing chain V4.56, the average values of the RA-2 S-Band backscattering parameter, shows an increase of ~0.65 dBs, the new S-band sigma0 being higher with respect to the previous versions.

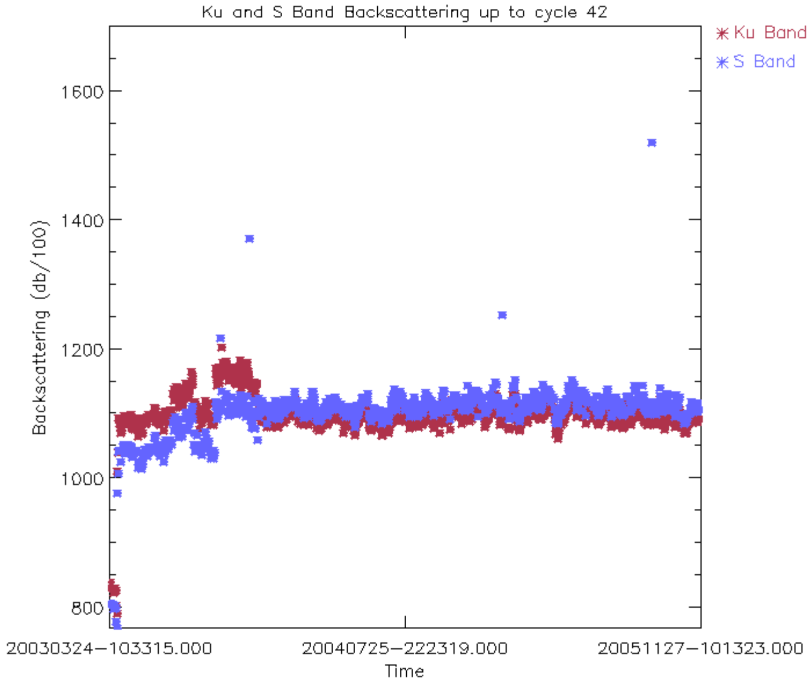

Figure 34: Ku and S band Backscattering daily averages up to cycle 42 (dB/100)

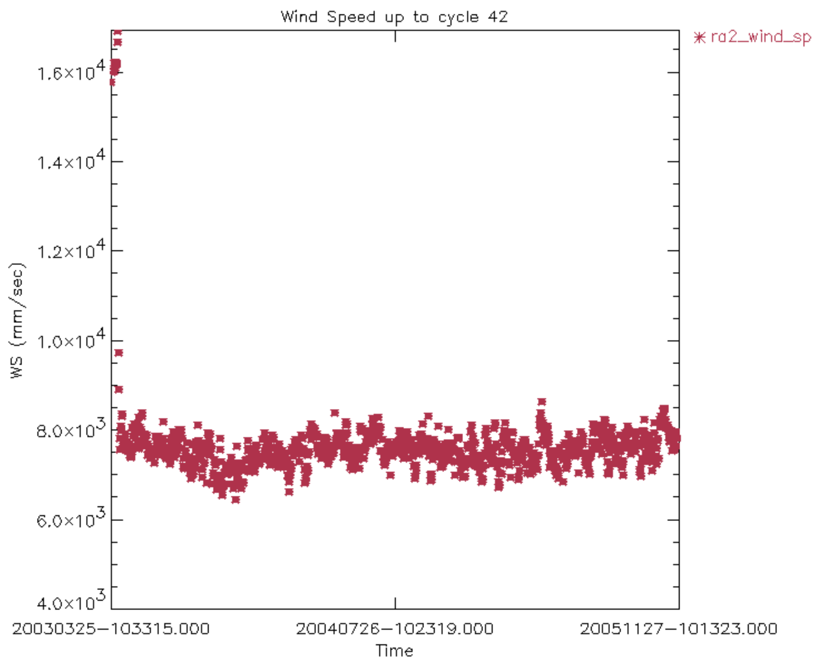

Figure 35: Wind Speed daily averages up to cycle 42 (mm/s)

8 PARTICULAR INVESTIGATIONS

During cycle 42 no special investigation has been performed.

APPENDIX 1: IPF UPGRADES

Table 4: L1B IPF version

IPF Version	Date of issue PDHS-K&E, LRAC	L1B Algortihm upgrades	L1B ADF updates	ADF filename
V4.53	Nov. 27, 2002			
V4.54	Apr. 7, 2003	*Wrong sign in AGC calibration estimation *Missing integrity check for the Data Block number read from the Level 0 Data Blocks *The altitude above CoG and the altitude rate have to be included in the records also in case of dummy records *1Hz data should be referenced to data block 9.5 not block 10	Correction of the Tx-Rx gain of Ku and S band parameters (3.5 dB)	RA2_CHD_AX
V4.56	Nov. 26, 2003	1- Extrapolation of AGC value to the Waveform center (49.5) for both Ku- and S-band. 2 - Correction for an error found in the evaluation of S band AGC.	RA2 IF Mask	RA2_IFF_AX
V4.57	PDHS-K: 29-04-2004 PDHS-E: 28-04-2004			
V4.58	Aug. 9, 2004			
V5.0.2	Oct. 24, 2005	MWR Side Lobe correction upgrade	- side lobe table and Config param	MWR_SLT_AX MWR_CON_AX
		USO clock period units correction	New ADF format - clock period un	RA2_USO_AX RA2_CHD_AX RA2_CON_AX
		RA-2 alignment: OBDH & USO datation, IE flags correction		
		Rain Flag tunning to compensate for the increase of the S band Sigma0	New table in SOI file	RA2_SOI_AX
		Monthly IF estimation		RA2_IFF_AX
		Level 1B S-Band anomaly flag	New format	RA2_CON_AX
		DORIS Navigator CFI upgrade (RA-2 & MWR)		

Table 5: L2 IPF version

PF Version	Date of issue PDHS	L2 Algortihm upgrades	L2 ADF updates	ADF filename
V4.53	Nov. 27, 2002			
V4.54	Apr. 7, 2003			
V4.56	Nov. 26, 2003	SPR 26 Tuning of the Ice2 retracking New MWR NN algorithm	MSS CLS01 Rain flag Updated OCOG retracker thresholds Ice1/Sea Ice Conf file Sea State Bias Table file GOT00.2 Ocean Tide Sol 1 Map file FES 2002 Ocean Tide Sol 2 Map file FES 2002 Tidal Loading Coeff Map	RA2_MSS_AX RA2_SOI_AX RA2_ICT_AX RA2_SSB_AX RA2_OT1_AX RA2_OT2_AX RA2_TLD_AX
V4.57	PDHS-K: 29-04-2004 PDHS-E: 28-04-2004	ECMWF meteo files handling		
V4.58	Aug. 9, 2004	Addition of a Pass Number Field in FD Level		
V5.0.2	Oct. 24, 2005	- Handling of the new RA2_CHD_AX ADF - Rain Flag tunning to compensate for the increase of the S band Sigma0 - Improving the mispointing estimation - Export of the Level 1B S-band flag into the Level 2 data product - Export of the Level 1B NRT orbit quality flag - Addition of a Pass Number Field in FD Level 2 SPH product - Addition of peakiness in Ku and S band in FDMAR - Addition of square of the SWH in Ku and S band - Correction of MCD flag - SPH pass number (field 8) set to 0 in SPH NRT Level 2 data products	New table in SOI file Two needed parameters in SOI file New format Addition of GOT2000.2 TLD New DEM AUX file (MACESS) merge of ACE land elevation data and Smith and Sandwell ocean bathymetry	RA2_CHD_AX RA2_SOI_AX RA2_SOI_AX RA2_SOI_AX RA2_TLG_AX AUX_DEM_AX

APPENDIX 2: AVAILABILITY

Table 6: RA-2 L0, L1b and L2 FGD Data products availability summary for cycle 42

Start orbit	Stop orbit	Time [msec] instrum. Unavail-ability	Time [msec] L0 gaps	Time [msec] L1b gaps	Time [msec] L2 (FGD) gaps	% instrum. avail.	% L0 avail.	% L1b avail.	% L2 (FGD) avail.
19093	19193	18.287.000	19.689.749	19.684.086	25.602.075	96.97	96.73	96.73	95.75
19193	19293	0	6.206.848	6.189.952	6.218.962	100	98.97	98.97	98.96
19293	19393	0	29.545.298	29.540.135	35.231.301	100	95.09	95.09	94.15
19393	19493	0	2.359.435	2.344.880	6.398.657	100	99.60	99.61	98.93
19493	19594	0	11.129.651	11.109.393	11.128.102	100	98.15	98.15	98.15

Table 7: MWR L0 Data products availability summary for cycle 42

Start orbit	Stop orbit	Time [sec] instrum. unavailability	Time [sec] L0 gaps	% instrum. avail.	% L0 avail.
19093	19193	0	71	100	99.988
19193	19293	0	11.064	100	98.170
19293	19393	0	28.753	100	95.245
19393	19493	0	1.320	100	99.781
19493	19594	0	10.368	100	98.285

Table 8: DORIS L0 Data products availability summary for cycle 42

Start orbit	Stop orbit	Time [sec] instrum. unavailability	Time [sec] L0 gaps	% instrum. avail.	% L0 avail.
19093	19193	0	7.586	100	99.372
19193	19293	0	12.562	100	98.961
19293	19393	0	61.016	100	94.955
19393	19493	0	4.270	100	99.646
19493	19594	0	22.505	100	98.139

Table 9: List of gaps for RA-2 L0 cycle 42

Start date	Start time	Stop date	Stop time	Duration [sec]	Start orbit	Stop orbit	Reason
24-oct-05	4.15.38	24-oct-05	4.16.56	78	19082	19082	PDS_UNKNOWN_FAILURE
24-oct-05	15.28.06	24-oct-05	15.29.23	77	19089	19089	PDS_UNKNOWN_FAILURE

25-oct-05	5.23.58	25-oct-05	5.25.16	78	19097	19097	PDS_UNKNOWN_FAILURE
25-oct-05	16.36.45	25-oct-05	16.38.03	78	19104	19104	PDS_UNKNOWN_FAILURE
26-oct-05	4.53.03	26-oct-05	4.54.21	78	19111	19111	PDS_UNKNOWN_FAILURE
26-oct-05	16.04.42	26-oct-05	16.06.00	78	19118	19118	PDS_UNKNOWN_FAILURE
27-oct-05	4.21.26	27-oct-05	4.22.44	78	19125	19125	PDS_UNKNOWN_FAILURE
27-oct-05	15.33.57	27-oct-05	15.35.15	78	19132	19132	PDS_UNKNOWN_FAILURE
28-oct-05	16.42.10	28-oct-05	16.43.27	77	19147	19147	PDS_UNKNOWN_FAILURE
28-oct-05	5.28.57	28-oct-05	5.34.13	316	19140	19140	PDS_UNKNOWN_FAILURE
28-oct-05	10.39.00	28-oct-05	10.40.05	65	19143	19143	PDS_UNKNOWN_FAILURE
28-oct-05	5.34.13	28-oct-05	10.39.00	18287	19140	19143	UNAV_RA2
29-oct-05	4.58.42	29-oct-05	4.59.59	77	19154	19154	PDS_UNKNOWN_FAILURE
29-oct-05	8.03.22	29-oct-05	8.03.29	7	19156	19156	PDS_UNKNOWN_FAILURE
29-oct-05	16.10.25	29-oct-05	16.11.43	78	19161	19161	PDS_UNKNOWN_FAILURE
31-oct-05	3.55.05	31-oct-05	3.56.23	78	19182	19182	PDS_UNKNOWN_FAILURE
31-oct-05	15.07.24	31-oct-05	15.08.42	78	19189	19189	PDS_UNKNOWN_FAILURE
01-nov-05	5.04.19	01-nov-05	5.05.36	77	19197	19197	PDS_UNKNOWN_FAILURE
01-nov-05	16.16.19	01-nov-05	16.17.37	78	19204	19204	PDS_UNKNOWN_FAILURE
02-nov-05	4.32.56	02-nov-05	4.34.14	78	19211	19211	PDS_UNKNOWN_FAILURE
02-nov-05	15.45.08	02-nov-05	15.46.26	78	19218	19218	PDS_UNKNOWN_FAILURE
03-nov-05	4.00.57	03-nov-05	4.02.15	78	19225	19225	PDS_UNKNOWN_FAILURE
03-nov-05	15.13.19	03-nov-05	15.14.37	78	19232	19232	PDS_UNKNOWN_FAILURE
03-nov-05	20.18.42	03-nov-05	21.30.57	4335	19235	19235	PDS_UNKNOWN_FAILURE
04-nov-05	5.09.55	04-nov-05	5.11.13	78	19240	19240	PDS_UNKNOWN_FAILURE
04-nov-05	16.22.14	04-nov-05	16.23.32	78	19247	19247	PDS_UNKNOWN_FAILURE
04-nov-05	5.07.43	04-nov-05	5.07.45	2	19240	19240	PDS_UNKNOWN_FAILURE
05-nov-05	4.35.40	05-nov-05	4.35.42	2	19254	19254	PDS_UNKNOWN_FAILURE
05-nov-05	4.38.41	05-nov-05	4.39.58	77	19254	19254	PDS_UNKNOWN_FAILURE
05-nov-05	15.47.55	05-nov-05	15.47.58	3	19261	19261	PDS_UNKNOWN_FAILURE
05-nov-05	15.50.43	05-nov-05	15.52.01	78	19261	19261	PDS_UNKNOWN_FAILURE
07-nov-05	5.13.19	07-nov-05	5.13.22	3	19283	19283	PDS_UNKNOWN_FAILURE
07-nov-05	5.15.32	07-nov-05	5.16.50	78	19283	19283	PDS_UNKNOWN_FAILURE
07-nov-05	16.28.08	07-nov-05	16.29.26	78	19290	19290	PDS_UNKNOWN_FAILURE
07-nov-05	19.56.32	07-nov-05	19.59.48	196	19292	19292	PDS_UNKNOWN_FAILURE
08-nov-05	4.44.25	08-nov-05	4.45.43	78	19297	19297	PDS_UNKNOWN_FAILURE
08-nov-05	15.53.40	08-nov-05	15.53.42	2	19304	19304	PDS_UNKNOWN_FAILURE
08-nov-05	15.56.19	08-nov-05	15.57.36	77	19304	19304	PDS_UNKNOWN_FAILURE
09-nov-05	4.12.41	09-nov-05	4.13.59	78	19311	19311	PDS_UNKNOWN_FAILURE
09-nov-05	15.22.24	09-nov-05	15.22.27	3	19318	19318	PDS_UNKNOWN_FAILURE
09-nov-05	15.25.08	09-nov-05	15.26.25	77	19318	19318	PDS_UNKNOWN_FAILURE
10-nov-05	5.21.09	10-nov-05	5.22.27	78	19326	19326	PDS_UNKNOWN_FAILURE
10-nov-05	16.34.02	10-nov-05	16.35.20	78	19333	19333	PDS_UNKNOWN_FAILURE

10-nov-05	22.54.25	10-nov-05	22.56.25	120	19336	19336	PDS_UNKNOWN_FAILURE
11-nov-05	4.50.10	11-nov-05	4.51.28	78	19340	19340	PDS_UNKNOWN_FAILURE
11-nov-05	16.01.54	11-nov-05	16.03.11	77	19347	19347	PDS_UNKNOWN_FAILURE
12-nov-05	4.18.33	12-nov-05	4.19.50	77	19354	19354	PDS_UNKNOWN_FAILURE
12-nov-05	15.31.02	12-nov-05	15.32.20	78	19361	19361	PDS_UNKNOWN_FAILURE
13-nov-05	22.58.30	14-nov-05	4.53.33	21303	19379	19383	PDS_UNKNOWN_FAILURE
14-nov-05	4.55.52	14-nov-05	6.54.17	7105	19383	19384	PDS_UNKNOWN_FAILURE
14-nov-05	16.07.29	14-nov-05	16.08.48	79	19390	19390	PDS_UNKNOWN_FAILURE
15-nov-05	4.24.17	15-nov-05	4.25.35	78	19397	19397	PDS_UNKNOWN_FAILURE
15-nov-05	15.33.41	15-nov-05	15.33.44	3	19404	19404	PDS_UNKNOWN_FAILURE
15-nov-05	15.36.43	15-nov-05	15.38.01	78	19404	19404	PDS_UNKNOWN_FAILURE
16-nov-05	3.52.08	16-nov-05	3.53.25	77	19411	19411	PDS_UNKNOWN_FAILURE
16-nov-05	16.44.50	16-nov-05	16.46.08	78	19419	19419	PDS_UNKNOWN_FAILURE
17-nov-05	5.01.28	17-nov-05	5.02.46	78	19426	19426	PDS_UNKNOWN_FAILURE
17-nov-05	16.13.20	17-nov-05	16.14.38	78	19433	19433	PDS_UNKNOWN_FAILURE
18-nov-05	4.26.44	18-nov-05	4.26.47	3	19440	19440	PDS_UNKNOWN_FAILURE
18-nov-05	4.30.01	18-nov-05	4.31.19	78	19440	19440	PDS_UNKNOWN_FAILURE
18-nov-05	15.39.19	18-nov-05	15.39.22	3	19447	19447	PDS_UNKNOWN_FAILURE
18-nov-05	15.42.18	18-nov-05	15.43.36	78	19447	19447	PDS_UNKNOWN_FAILURE
19-nov-05	3.55.57	19-nov-05	3.55.59	2	19454	19454	PDS_UNKNOWN_FAILURE
19-nov-05	3.57.59	19-nov-05	3.59.17	78	19454	19454	PDS_UNKNOWN_FAILURE
19-nov-05	15.10.19	19-nov-05	15.11.37	78	19461	19461	PDS_UNKNOWN_FAILURE
21-nov-05	4.35.46	21-nov-05	4.37.03	77	19483	19483	PDS_UNKNOWN_FAILURE
21-nov-05	15.45.00	21-nov-05	15.45.03	3	19490	19490	PDS_UNKNOWN_FAILURE
21-nov-05	15.47.53	21-nov-05	15.49.11	78	19490	19490	PDS_UNKNOWN_FAILURE
21-nov-05	17.36.17	21-nov-05	17.57.16	1259	19491	19491	PDS_UNKNOWN_FAILURE
22-nov-05	4.03.51	22-nov-05	4.05.08	77	19497	19497	PDS_UNKNOWN_FAILURE
22-nov-05	15.16.13	22-nov-05	15.17.31	78	19504	19504	PDS_UNKNOWN_FAILURE
23-nov-05	5.10.28	23-nov-05	5.10.31	3	19512	19512	PDS_UNKNOWN_FAILURE
23-nov-05	5.12.41	23-nov-05	5.13.59	78	19512	19512	PDS_UNKNOWN_FAILURE
23-nov-05	16.25.08	23-nov-05	16.26.26	78	19519	19519	PDS_UNKNOWN_FAILURE
24-nov-05	4.41.30	24-nov-05	4.42.48	78	19526	19526	PDS_UNKNOWN_FAILURE
24-nov-05	15.50.44	24-nov-05	15.50.47	3	19533	19533	PDS_UNKNOWN_FAILURE
24-nov-05	15.53.28	24-nov-05	15.54.46	78	19533	19533	PDS_UNKNOWN_FAILURE
24-nov-05	4.38.35	24-nov-05	4.38.37	2	19526	19526	PDS_UNKNOWN_FAILURE
25-nov-05	4.09.42	25-nov-05	4.11.00	78	19540	19540	PDS_UNKNOWN_FAILURE
25-nov-05	15.19.32	25-nov-05	15.19.35	3	19547	19547	PDS_UNKNOWN_FAILURE
25-nov-05	15.22.07	25-nov-05	15.23.25	78	19547	19547	PDS_UNKNOWN_FAILURE
26-nov-05	5.16.04	26-nov-05	5.16.07	3	19555	19555	PDS_UNKNOWN_FAILURE
26-nov-05	5.18.17	26-nov-05	5.19.35	78	19555	19555	PDS_UNKNOWN_FAILURE
26-nov-05	16.31.02	26-nov-05	16.32.20	78	19562	19562	PDS_UNKNOWN_FAILURE

26-nov-05	19.57.56	26-nov-05	20.15.47	1071	19564	19564	PDS_UNKNOWN_FAILURE
26-nov-05	20.20.48	26-nov-05	22.50.00	8952	19564	19565	PDS_UNKNOWN_FAILURE
27-nov-05	4.47.14	27-nov-05	4.48.32	78	19569	19569	PDS_UNKNOWN_FAILURE

Table 10: List of gaps for MWR L0 cycle 42

Start date	Start time	Stop date	Stop time	Duration [sec]	Start orbit	Stop orbit	Reason
29-oct-05	8.02.20	29-oct-05	8.03.32	72	19156	19156	PDS_UNKNOWN_FAILURE
03-nov-05	20.17.45	03-nov-05	21.30.57	4392	19235	19235	PDS_UNKNOWN_FAILURE
07-nov-05	19.55.30	07-nov-05	19.59.30	240	19292	19292	PDS_UNKNOWN_FAILURE
10-nov-05	22.53.37	10-nov-05	22.56.25	168	19336	19336	PDS_UNKNOWN_FAILURE
13-nov-05	22.57.44	14-nov-05	6.54.09	28585	19379	19384	PDS_UNKNOWN_FAILURE
21-nov-05	17.35.14	21-nov-05	17.57.14	1320	19491	19491	PDS_UNKNOWN_FAILURE
26-nov-05	19.57.01	26-nov-05	22.49.50	10369	19564	19565	PDS_UNKNOWN_FAILURE

Table 11: List of gaps for RA-2 L1b cycle 42

Start date	Start time	Stop date	Stop time	Duration [sec]	Start orbit	Stop orbit	Reason
24-oct-05	4.15.38	24-oct-05	4.16.56	78	19082	19082	PDS_UNKNOWN_FAILURE
24-oct-05	15.28.06	24-oct-05	15.29.23	77	19089	19089	PDS_UNKNOWN_FAILURE
25-oct-05	5.23.58	25-oct-05	5.25.16	78	19097	19097	PDS_UNKNOWN_FAILURE
25-oct-05	16.36.45	25-oct-05	16.38.03	78	19104	19104	PDS_UNKNOWN_FAILURE
26-oct-05	4.53.03	26-oct-05	4.54.21	78	19111	19111	PDS_UNKNOWN_FAILURE
26-oct-05	16.04.42	26-oct-05	16.06.00	78	19118	19118	PDS_UNKNOWN_FAILURE
27-oct-05	4.21.26	27-oct-05	4.22.44	78	19125	19125	PDS_UNKNOWN_FAILURE
27-oct-05	15.33.57	27-oct-05	15.35.15	78	19132	19132	PDS_UNKNOWN_FAILURE
28-oct-05	5.34.13	28-oct-05	10.39.00	18287	19140	19143	UNAV_RA2
28-oct-05	16.42.10	28-oct-05	16.43.27	77	19147	19147	PDS_UNKNOWN_FAILURE
28-oct-05	5.28.57	28-oct-05	5.34.13	316	19140	19140	PDS_UNKNOWN_FAILURE
28-oct-05	10.39.00	28-oct-05	10.40.05	65	19143	19143	PDS_UNKNOWN_FAILURE
29-oct-05	4.58.42	29-oct-05	4.59.59	77	19154	19154	PDS_UNKNOWN_FAILURE
29-oct-05	4.59.59	29-oct-05	5.00.00	1	19154	19154	PDS_UNKNOWN_FAILURE
29-oct-05	8.03.24	29-oct-05	8.03.29	5	19156	19156	PDS_UNKNOWN_FAILURE
29-oct-05	16.10.25	29-oct-05	16.11.43	78	19161	19161	PDS_UNKNOWN_FAILURE
31-oct-05	3.55.05	31-oct-05	3.56.23	78	19182	19182	PDS_UNKNOWN_FAILURE
31-oct-05	15.07.24	31-oct-05	15.08.42	78	19189	19189	PDS_UNKNOWN_FAILURE
01-nov-05	5.04.19	01-nov-05	5.05.36	77	19197	19197	PDS_UNKNOWN_FAILURE
01-nov-05	16.16.19	01-nov-05	16.17.37	78	19204	19204	PDS_UNKNOWN_FAILURE
02-nov-05	4.32.56	02-nov-05	4.34.14	78	19211	19211	PDS_UNKNOWN_FAILURE
02-nov-05	15.45.08	02-nov-05	15.46.26	78	19218	19218	PDS_UNKNOWN_FAILURE

03-nov-05	4.00.57	03-nov-05	4.02.15	78	19225	19225	PDS_UNKNOWN_FAILURE
03-nov-05	15.13.19	03-nov-05	15.14.37	78	19232	19232	PDS_UNKNOWN_FAILURE
03-nov-05	20.18.43	03-nov-05	21.30.57	4334	19235	19235	PDS_UNKNOWN_FAILURE
04-nov-05	16.22.14	04-nov-05	16.23.32	78	19247	19247	PDS_UNKNOWN_FAILURE
04-nov-05	5.09.55	04-nov-05	5.11.13	78	19240	19240	PDS_UNKNOWN_FAILURE
05-nov-05	4.38.41	05-nov-05	4.39.58	77	19254	19254	PDS_UNKNOWN_FAILURE
05-nov-05	15.50.43	05-nov-05	15.52.01	78	19261	19261	PDS_UNKNOWN_FAILURE
07-nov-05	5.15.32	07-nov-05	5.16.50	78	19283	19283	PDS_UNKNOWN_FAILURE
07-nov-05	16.28.08	07-nov-05	16.29.26	78	19290	19290	PDS_UNKNOWN_FAILURE
07-nov-05	19.56.33	07-nov-05	19.59.48	195	19292	19292	PDS_UNKNOWN_FAILURE
08-nov-05	4.44.25	08-nov-05	4.45.43	78	19297	19297	PDS_UNKNOWN_FAILURE
08-nov-05	15.56.19	08-nov-05	15.57.36	77	19304	19304	PDS_UNKNOWN_FAILURE
09-nov-05	4.12.41	09-nov-05	4.13.59	78	19311	19311	PDS_UNKNOWN_FAILURE
09-nov-05	15.22.25	09-nov-05	15.22.27	2	19318	19318	PDS_UNKNOWN_FAILURE
09-nov-05	15.25.08	09-nov-05	15.26.25	77	19318	19318	PDS_UNKNOWN_FAILURE
10-nov-05	22.54.26	10-nov-05	22.56.25	119	19336	19336	PDS_UNKNOWN_FAILURE
10-nov-05	5.21.09	10-nov-05	5.22.27	78	19326	19326	PDS_UNKNOWN_FAILURE
10-nov-05	16.34.02	10-nov-05	16.35.20	78	19333	19333	PDS_UNKNOWN_FAILURE
11-nov-05	4.50.10	11-nov-05	4.51.28	78	19340	19340	PDS_UNKNOWN_FAILURE
11-nov-05	16.01.54	11-nov-05	16.03.11	77	19347	19347	PDS_UNKNOWN_FAILURE
12-nov-05	4.18.33	12-nov-05	4.19.50	77	19354	19354	PDS_UNKNOWN_FAILURE
12-nov-05	15.31.02	12-nov-05	15.32.20	78	19361	19361	PDS_UNKNOWN_FAILURE
13-nov-05	22.58.31	14-nov-05	4.53.33	21302	19379	19383	PDS_UNKNOWN_FAILURE
14-nov-05	4.55.52	14-nov-05	6.54.17	7105	19383	19384	PDS_UNKNOWN_FAILURE
14-nov-05	16.07.29	14-nov-05	16.08.48	79	19390	19390	PDS_UNKNOWN_FAILURE
15-nov-05	4.24.17	15-nov-05	4.25.35	78	19397	19397	PDS_UNKNOWN_FAILURE
15-nov-05	15.36.43	15-nov-05	15.38.01	78	19404	19404	PDS_UNKNOWN_FAILURE
16-nov-05	3.52.08	16-nov-05	3.53.25	77	19411	19411	PDS_UNKNOWN_FAILURE
16-nov-05	16.44.50	16-nov-05	16.46.08	78	19419	19419	PDS_UNKNOWN_FAILURE
17-nov-05	5.01.28	17-nov-05	5.02.46	78	19426	19426	PDS_UNKNOWN_FAILURE
17-nov-05	16.13.20	17-nov-05	16.14.38	78	19433	19433	PDS_UNKNOWN_FAILURE
18-nov-05	15.42.18	18-nov-05	15.43.36	78	19447	19447	PDS_UNKNOWN_FAILURE
18-nov-05	4.30.01	18-nov-05	4.31.19	78	19440	19440	PDS_UNKNOWN_FAILURE
19-nov-05	3.57.59	19-nov-05	3.59.17	78	19454	19454	PDS_UNKNOWN_FAILURE
19-nov-05	15.10.19	19-nov-05	15.11.37	78	19461	19461	PDS_UNKNOWN_FAILURE
21-nov-05	4.35.46	21-nov-05	4.37.03	77	19483	19483	PDS_UNKNOWN_FAILURE
21-nov-05	15.47.53	21-nov-05	15.49.11	78	19490	19490	PDS_UNKNOWN_FAILURE
21-nov-05	17.36.19	21-nov-05	17.57.16	1257	19491	19491	PDS_UNKNOWN_FAILURE
22-nov-05	4.03.51	22-nov-05	4.05.08	77	19497	19497	PDS_UNKNOWN_FAILURE
22-nov-05	15.16.13	22-nov-05	15.17.31	78	19504	19504	PDS_UNKNOWN_FAILURE
23-nov-05	5.12.41	23-nov-05	5.13.59	78	19512	19512	PDS_UNKNOWN_FAILURE

23-nov-05	16.25.08	23-nov-05	16.26.26	78	19519	19519	PDS_UNKNOWN_FAILURE
24-nov-05	4.41.30	24-nov-05	4.42.48	78	19526	19526	PDS_UNKNOWN_FAILURE
24-nov-05	15.53.28	24-nov-05	15.54.46	78	19533	19533	PDS_UNKNOWN_FAILURE
25-nov-05	15.22.07	25-nov-05	15.23.25	78	19547	19547	PDS_UNKNOWN_FAILURE
25-nov-05	4.09.42	25-nov-05	4.11.00	78	19540	19540	PDS_UNKNOWN_FAILURE
26-nov-05	5.16.05	26-nov-05	5.16.07	2	19555	19555	PDS_UNKNOWN_FAILURE
26-nov-05	5.18.17	26-nov-05	5.19.35	78	19555	19555	PDS_UNKNOWN_FAILURE
26-nov-05	16.31.02	26-nov-05	16.32.20	78	19562	19562	PDS_UNKNOWN_FAILURE
26-nov-05	19.57.57	26-nov-05	20.15.47	1070	19564	19564	PDS_UNKNOWN_FAILURE
26-nov-05	20.20.53	26-nov-05	22.50.00	8947	19564	19565	PDS_UNKNOWN_FAILURE
27-nov-05	4.47.14	27-nov-05	4.48.32	78	19569	19569	PDS_UNKNOWN_FAILURE

APPENDIX 3: LEVEL 2 STATIC AUXILIARY DATA FILES

AUX_DEM_AXVIEC20031201_000000_20031201_000000_20200101_000000
MWR_LSF_AXVIEC20020313_172218_20020101_000000_20200101_000000
RA2_CHD_AXVIEC20051017_093900_20020101_000000_20200101_000000
RA2_CST_AXVIEC20020621_135858_20020101_000000_20200101_000000
RA2_DIP_AXVIEC20020122_134206_20020101_000000_20200101_000000
RA2_GEO_AXVIEC20020314_093428_20020101_000000_20200101_000000
RA2_ICT_AXVIEC20031208_143628_20020101_000000_20200101_000000
RA2_IOC_AXVIEC20020122_141121_20020101_000000_20200101_000000
RA2_MET_AXVIEC20020204_073357_20020101_000000_20200101_000000
RA2_MSS_AXVIEC20031208_145545_20020101_000000_20200101_000000
RA2_OT1_AXVIEC20040120_082051_20020101_000000_20200101_000000
RA2_OT2_AXVIEC20031208_150159_20020101_000000_20200101_000000
RA2_SET_AXVIEC20020122_150917_20020101_000000_20200101_000000
RA2_SL1_AXVIEC20030131_100228_20020101_000000_20200101_000000
RA2_SL2_AXVIEC20030131_101757_20020101_000000_20200101_000000
RA2_SOI_AXVIEC20051003_170000_20020101_000000_20200101_000000
RA2_SSB_AXVIEC20031208_150749_20020101_000000_20200101_000000
RA2_TLD_AXVIEC20031208_151137_20020101_000000_20200101_000000
RA2_TLG_AXVIEC20040310_110000_20020101_000000_20200101_000000

APPENDIX 4: SIGMA0 ABSOLUTE CALIBRATION

Table 12: Transponder measurement results up to cycle 42

Absolute Orbit nb	Date of Measurement	Location / Rel. track	RA-2 resolution	Transponder Bias [dB]	ECMWF Wet Tropo. Corr. [dB]
10389	24-feb-04	Rome / 315	Low	1,552	0,120
10511	04-mar-04	Valmontone / 437	Low	1,542	0,102
10618	11-mar-04	Fiuggi / 43	Low	1,447	0,135
10783	23-mar-04	Maccarese / 208	Low	1,540	0,142
10890	30-mar-04	Rome / 315	Low	1,442	0,152
11119	15-apr-04	Fiuggi / 43	High	0,963	0,122
11513	13-mag-04	Valmontone / 437	Low	1,353	0,133
11620	20-mag-04	Fiuggi / 43	Low	1,427	0,139
11892	08-giu-04	Rome / 315	Low	1,504	0,154
12014	17-giu-04	Valmontone / 437	Low	1,448	0,348
12121	24-giu-04	Fiuggi / 43	Low	1,576	0,149
14290	23-nov-04	Maccarese / 208	Low	1,43	0,164
14397	30-nov-04	Rome / 315	Low	1,11	0,142
14519	9-dic-04	Valmontone / 437	Low	1,26	0,248
14791	28-dic-04	Maccarese / 208	High	0,97	0,134
14898	4-gen-05	Rome / 315	High	0,95	0,114
15020	13-gen-05	Valmontone / 437	High	0,88	0,118
15127	20-gen-05	Fiuggi / 43	High	1,01	0,108
15292	1-feb-05	Maccarese / 208	High	0,95	0,132
15399	8-feb-05	Rome / 315	High	1,05	0,124
15521	17-feb-05	Valmontone / 437	High	0,94	0,115
15793	8-mar-05	Maccarese / 208	High	0,93	0,116
15900	15-mar-05	Rome / 315	High	0,93	0,128
16022	24-mar-05	Valmontone / 437	High	0,94	0,154
16294	12-apr-05	Maccarese / 208	High	0,97	0,140
16401	19-apr-05	Rome / 315	High	0,99	0,134
16523	28-apr-05	Valmontone / 437	High	0,97	0,114
16795	17-may-05	Maccarese / 208	High	0,84	0,168
16902	24-may-05	Rome / 315	High	1,00	0,152
17403	28-jun-05	Rome / 315	High	1,13	0,16
17525	7-jul-05	Valmontone / 437	High	1,04	0,13
17904	02-aug-05	Rome / 315	High	1,02	0,188
18026	11-aug-05	Valmontone / 437	High	0,93	0,154
18405	06-sep-05	Rome / 315	High	1,06	0,16
18634	22-Sep-05	Fiuggi/43	High	1,00	0,076
18799	04-Oct-05	Maccarese/208	High	0,85	0,082
18906	11-Oct-05	Perm site Rome / 315	Low	1.46	0,078
19407	15-Nov-2005	Perm site Rome / 315	High	1.09	0,095

APPENDIX 5: S-BAND ANOMALY

Table 13: List of L2 FGD Files affected by S-Band anomaly during cycle 42

File name	Start date	Start time	Stop date	Stop time
RA2_FGD_2PNPDK20051107_071520_000039702042_00192_19284_1357.N1	07-nov-05	07:15:20	07-nov-05	08:21:30
RA2_FGD_2PNPDK20051107_082033_000062542042_00193_19285_1358.N1	07-nov-05	08:20:33	07-nov-05	10:04:47
RA2_FGD_2PNPDK20051107_100350_000059902042_00194_19286_1359.N1	07-nov-05	10:03:50	07-nov-05	11:43:40
RA2_FGD_2PNPDK20051107_114242_000059652042_00195_19287_1360.N1	07-nov-05	11:42:42	07-nov-05	13:22:08
RA2_FGD_2PNPDK20051107_132110_000059302042_00196_19288_1361.N1	07-nov-05	13:21:10	07-nov-05	15:00:00
RA2_FGD_2PNPDK20051107_145848_000052032042_00197_19289_1362.N1	07-nov-05	14:58:48	07-nov-05	16:25:32
RA2_FGD_2PNPDK20051113_195955_000000342042_00286_19378_1442.N1	13-nov-05	19:59:55	13-nov-05	20:00:29
RA2_FGD_2PNPDK20051114_080123_000061042042_00293_19385_1447.N1	14-nov-05	08:01:23	14-nov-05	09:43:06
RA2_FGD_2PNPDK20051114_094200_000061102042_00294_19386_1448.N1	14-nov-05	09:42:00	14-nov-05	11:23:50
RA2_FGD_2PNPDK20051114_112241_000060622042_00295_19387_1449.N1	14-nov-05	11:22:41	14-nov-05	13:03:43
RA2_FGD_2PNPDK20051114_130244_000058952042_00296_19388_1450.N1	14-nov-05	13:02:44	14-nov-05	14:40:59
RA2_FGD_2PNPDK20051115_123037_000059882042_00310_19402_1462.N1	15-nov-05	12:30:37	15-nov-05	14:10:25